New insights into the thermal regime and hydrodynamics of the early Late Cretaceous Arctic

ROBERT SPICER [1,2*], PAUL VALDES[3], ALICE HUGHES[2], JIAN YANG[4], TERESA SPICER[4], ALEXEI HERMAN[5], ALEXANDER FARNSWORTH[3]

[1]School of Environment, Earth and Ecosystem Sciences, The Open University, Milton Keynes, MK7 6AA, UK.

[2]Xishuangbanna Tropical Botanical Garden, Chinese Academy of Sciences, Menglun, Mengla, Yunnan 666303, P.R. China.

[3]School of Geographical Sciences, University of Bristol, Bristol BS81SS, UK.

[4] State Key Laboratory of Systematic and Evolutionary Botany, Institute of Botany, Chinese Academy of Sciences, Beijing 100093, P.R. China.

[5]Geological Institute, Russian Academy of Sciences, Moscow 119017, Russia.

• Corresponding author: r.a.spicer@open.ac.uk

Keywords: Polar warmth, palaeoclimate, CLAMP, ecosystem, Alaska, Russia, plant fossils

Abstract – The Arctic is warming faster than anywhere else of comparable size on Earth, impacting global climate feedbacks and the Arctic biota. However, a warm Arctic is not novel. The Late Cretaceous fossil record of the region enables a detailed reconstruction of polar environmental conditions, and a thriving extinct ecosystem, during a previous 'hothouse' global climate. Using leaf form (physiognomy) and tree ring characteristics we reconstruct Cenomanian to Coniacian polar thermal and hydrological regimes over an average annual cycle at eight locations in north-eastern Russia and northern Alaska. A new high spatial resolution (~1 km) WorldClim2 calibration of the Climate-Leaf Analysis Multivariate Program (CLAMP) yields similar, but often slightly warmer, results to previous analyses, but also provides more detailed insights into the hydrological regime through the return of annual and seasonal vapour pressure deficit (VPD), potential evapotranspiration (PET) estimates and soil moisture, as well as new thermal overviews through measures of thermicity and growing degree days. The new results confirm the overall warmth of the region, particularly close to the Arctic ocean, but reveals strong local differences that may be related to palaeoelevation in the Okhotsk-Chukotka Volcanogenic Belt in north-eastern Russia. While rainfall estimates have large uncertainties due to year-round wet soils in most locations, new measures of VPD and PET show persistent high humidity, but with notably drier summers at all the Arctic sites.

1. Introduction

The Arctic is warming faster than almost all other parts of our planet (IPCC 2014). This phenomenon is consistent with 'polar amplification' (Lee 2014) where any change in planetary scale net radiation balance, irrespective of whether ice is present at the poles or not, produces larger temperature changes at higher latitudes than in equatorial regions. Polar amplification is no better illustrated than in the Arctic during past episodes of extreme

Deleted: and t

warmth, such as in the early Late Cretaceous. Polar amplification makes Arctic palaeoclimate proxies sensitive recorders of global change phenomena, and by studying warm Arctic conditions we can derive the most reliable insights into future climate, and linked biospheric responses, at high northern latitudes.

The current warming of the Arctic is dramatic and perhaps inevitably most investigations into the Late Cretaceous palaeoclimate of the region have focussed on the ancient thermal regime (e.g. Spicer & Parrish 1986; Spicer & Corfield 1992; Herman & Spicer 1996a, 1997a; Amiot et al. 2004; Spicer & Herman 2010; Herman, Spicer & Spicer 2016), but arguably more important is the polar hydrological cycle. In today's 'coldhouse' world a strong polar high-pressure cell leads to a relatively dry Arctic and only low temperatures, and thus low evaporation, prevents widespread aridity. However, in a warmer world a weaker polar high, and thus a weaker polar front, would have profound implications for global atmospheric circulation (including phenomena such as polar vortex outbreaks) and the water cycle.

It is possible that in the Late Cretaceous a warm Arctic Ocean generated vigorous ocean-atmosphere feedbacks that helped sustain that ocean warmth while also producing a more or less permanent Arctic cloud cap (Spicer et al. 2014), but atmospheric hydrology is poorly constrained through a lack of reliable proxies. The focus of this work is to re-examine the Arctic early Late Cretaceous climate and introduce new quantitative proxy palaeo-humidity measurements in order to characterise better the polar environment at times of global warmth.

Late Cretaceous Arctic sediments of Alaska and north-eastern Russia, collectively referred to here as the North Pacific Region (NPR) (Fig. 1), host a wealth of palaeontological evidence attesting to a highly diverse extinct ecosystem thriving under a temperate and humid climate at palaeolatitudes as high as 82 °N (Fig. 2). The rich plant fossil record from the NPR

has been investigated for more than a century (see background reviews in http://arcticfossils.nsii.org.cn) and is well documented in a large body of work (e.g. Hollick 1930; Samylina 1963; Lebedev 1965; Smiley 1966; Budantsev 1968; Samylina 1968; Smiley 1969a, b; Samylina 1973; Samylina 1974a, b; Filippova 1975a, b; Krassilov 1975; Lebedev 1976; Samylina 1976; Kiritchkova & Samylina 1978; Krassilov 1978; Filippova 1979; Scott & Smiley 1979; Detterman & Spicer 1981; Budantsev 1983; Spicer & Parrish 1986; Spicer 1986; Lebedev 1987; Spicer, Wolfe & Nichols 1987; Spicer 1987; Filippova 1988; Golovneva 1988; Grant, Spicer & Parrish 1988; Parrish & Spicer 1988a, b; Samylina 1988; Filippova 1989; Lebedev & Herman 1989; Herman 1990; Spicer & Chapman 1990; Spicer & Parrish 1990a; Spicer & Parrish 1990b; Golovneva 1991a, b; Herman 1991; Herman & Lebedev 1991; Herman & Shczepetov 1991; Samylina & Shczepetov 1991; Shczepetov 1991; Golovneva & Herman 1992; Lebedev 1992; Shczepetov, Herman & Belaya 1992; Spicer & Corfield 1992; Spicer, Parrish & Grant 1992; Filippova & Abramova 1993; Herman 1993; Spicer, Rees & Chapman 1993; Filippova 1994; Golovneva 1994a, b; Herman 1994; Herman & Spicer 1995; Shczepetov 1995; Herman & Spicer 1996b; Herman & Spicer 1997a, b; Golovneva 2000; Herman 2002; Herman, Spicer & Kvacek 2002; Spicer et al. 2002; Craggs 2005; Herman 2007; Herman et al. 2009; Golovneva & Alekseev 2010; Spicer & Herman 2010; Tomsich et al. 2010; Golovneva, Shchepetov & Alekseev 2011; Herman 2011, 2013; Alekseev, Herman & Shchepetov 2014; Shczepetov & Golovneva 2014; Golovneva, Herman & Shczepetov 2015; Golovneva & Shchepetov 2015; Herman et al. 2016; Herman, Spicer & Spicer 2016; Herman & Solokova 2016; Vasilenko, Maslova & Herman 2016; Shczepetov & Herman 2017; Nikitenko et al. 2017, 2018; Herman et al. 2019). While not exhaustive, these works attest to the richness and intensity of study that the Cretaceous Arctic floras have attracted despite the logistic difficulties of working in remote regions. A brief synthesis is given here.

Deleted: Samylina 1974b;
Deleted: 1975b
Deleted: Filippova 1975a;
Deleted: a
Deleted: et al.
Deleted: et al.
Deleted: Parrish & Spicer 1988b;
Formatted: Highlight
Deleted: a
Deleted: et al.
Formatted: Highlight
Deleted: Golovneva 1994a;
Deleted: et al.
Deleted: so only
Deleted: a
Deleted: overview

[Figure 1 near here]

[Figure 2 near here]

1.a. Early Late Cretaceous Arctic Forests

In the early Late Cretaceous at latitudes above the palaeo-Arctic Circle (~66 °N) forests were conifer-dominated and at high latitudes almost exclusively deciduous (Parrish & Spicer 1988b; Spicer & Parrish 1990b; Spicer & Herman 2001; Spicer et al. 2002; Spicer & Herman 2010; Herman, Spicer & Spicer 2016). Key canopy-forming taxa were predominantly *Cephalotaxopsis, Elatocladus, Pityophyllum, Araucarites, Sequoia reichenbachii* and *Pagiophyllum*, while angiosperms were most abundant as understorey elements and along stream sides (Spicer & Herman 2010; Herman, Spicer & Spicer 2016), but were non-existent or rare in swamp or mire forests (Spicer, Parrish & Grant 1992). Evergreen elements were regionally comparatively rare and restricted to conifers such as *Araucarites, Pagiophyllum* and *Geinitzia* (http://arcticfossils.nsii.org.cn) characterised by having small hook- and scale-like xeromorphic leaves that reduced water loss during winter dormancy. Ground cover consisted mostly of ferns and sphenophytes (Herman, Spicer & Spicer 2016), but towards the end of the Late Cretaceous, even at the highest latitudes, herbaceous angiosperms (probably annuals and preserved only as pollen) contributed to the ground cover especially in areas disturbed by wildfires or along river margins (Frederiksen, Ager & Edwards 1988; Herman, Spicer & Spicer 2016). A comprehensive illustrated catalogue of Late Cretaceous polar forest megafossils is available online at http://arcticfossils.nsii.org.cn.

Preserved standing isolated trees (Herman, Spicer & Spicer 2016) and even “fossil forests” are not uncommon in Late Cretaceous floodplain successions of the NPR. Stands of

Deleted:

Formatted: Not Highlight

Deleted: et al.

Formatted: Not Highlight

straight upright trunks up to 4.5 m tall and 0.7 m in diameter have been reported from northern Alaska (Decker et al. 1997) and evidence that these represent mire forests comes from the observation they are rooted in coals and carbonaceous mudstones. These standing trees attest not only to the stature, and structure of the mire forests, but periodic extremely high sedimentation rates, suggesting intense rainfall events, river channel breakouts and associated flooding.

Occasionally fossil wood is structurally preserved and to-date all wood specimens recovered have been coniferous with well-developed growth rings, typically showing sharp transitions between summer growth and winter dormancy (Parrish & Spicer 1988a; Spicer & Parrish 1990a; Herman, Spicer & Spicer 2016). Summer-wood rings in Cenomanian age trees tend to be wide with typically >100 cells produced each growing season and few false rings (Parrish & Spicer 1988a; Herman, Spicer & Spicer 2016) showing that growth was largely uninterrupted during the summer season, but Maastrichtian woods have narrow early (summer) rings with few smaller cells and numerous false rings indicative of frequent interruptions to growth, most likely caused by temperatures falling below 10 °C (Spicer & Parrish 1990a; Spicer & Herman 2010; Herman, Spicer & Spicer 2016).

1.b. Insolation and General Thermal Regime

As far as can be determined Earth's rotational and magnetic poles were roughly coincidental in the Late Cretaceous and obliquity, and thus the high latitude light regime, was similar to that of today (Lottes 1987) meaning that Arctic winters in near-polar settings were characterised by several months of darkness (Figs. 3–5). Despite this lack of direct insolation polar winters along the coastlines of the Arctic Ocean were surprisingly warm, experiencing temperatures that remained above freezing for much of the time (Spicer & Parrish 1990b; Herman & Spicer 1996a, 1997a; Herman, Spicer & Spicer 2016). While the temperature

Deleted: 2

Formatted: Font color: Custom Color(RGB(142,170,219))

Deleted: 4

Formatted: Font color: Custom Color(RGB(142,170,219))

Formatted: Font color: Custom Color(RGB(142,170,219))

regime of the Late Cretaceous Arctic has been well characterised through multiple proxies, the hydrological system is less well constrained.

1.c. Research Scope

In this work we re-examine the thermal regime of this extinct early Late Cretaceous (Cenomanian to Coniacian) polar 'Lost World' in the light of new high spatial resolution (~1 km) WorldClim2 (Fick & Hijmans 2017; http://www.worldclim.org/) calibrations of the non-taxonomic leaf physiognomic proxy known as CLAMP (http://clamp.ibcas.ac.cn), but the main focus is to explore new insights into the hydrological regime. We examine not only precipitation and soil moisture capacity, but humidity in terms of specific humidity (SH), relative humidity (RH), vapour pressure deficit (VPD) and potential evapotranspiration (PET). VPD and PET are investigated in respect of annual average values and seasonal variations.

2. Methods and Materials

Individual plants are spatially static so they have to be well adapted to their local environment or they die as a direct result of environmental stress or competition from those better equipped to withstand the prevailing conditions. These adaptations, preserved in the abundant early Late Cretaceous plant fossil record of the NPR, can be used to determine past conditions either as average annual or seasonal climate, as in the case of leaf form, or as a near-daily record of environmental change encoded as variations in wood growth (tree rings). By using both leaf form and tree ring data (Herman, Spicer & Spicer 2016) we can quantify the early Late Cretaceous high Arctic atmospheric conditions over seasonal or even sub-seasonal temporal resolutions.

Deleted:)
Deleted:)
Deleted: down to a
Deleted:
Deleted: measured in weeks (Herman et al. 2016)

192 The principal leaf-based palaeoclimate proxy for assessing a range of climate
193 variables is known as CLAMP (Climate-Leaf Analysis Multivariate Program)
194 (http://clamp.ibcas.ac.cn) (Wolfe 1993; Kovach & Spicer 1996; Yang et al. 2011, 2015).
195 CLAMP utilises the universal relationships that exist between leaf form in woody
196 dicotyledonous plants and an array of climate variables. On a global scale aggregate leaf form
197 in a stand of vegetation is more strongly determined by climate than by taxonomic
198 composition (Yang et al. 2015), and through a combination of pleiotropy and integrated
199 developmental pathways all leaf traits are correlated with each other (Pigliucci 2003) and an
200 array of climate variables (Wolfe 1993; Wolfe & Spicer 1999; Yang et al. 2011, 2015). Using
201 a multivariate statistical engine CLAMP decodes these relationships and, by scoring fossil
202 leaf traits the same way as for living vegetation growing under known climatic regimes,
203 estimates of past conditions can be obtained (http://clamp.ibcas.ac.cn).
204 No proxy is perfect, so a multiproxy approach should be used where possible. For the
205 high Late Cretaceous Arctic CLAMP and oxygen isotopes from marine (Zakharov et al.
206 1999, 2011) and non-marine vertebrate remains (Amiot et al. 2004) all give broadly similar
207 estimates (Herman & Spicer 1997a; Amiot et al. 2004; Spicer & Herman 2010; Herman,
208 Spicer & Spicer 2016), increasing confidence in the fidelity of all the proxies. However, all
209 proxies depend on modern observations for their calibration and several modern
210 observational datasets are available, each with its own characteristics.
211
212 **2.a. CLAMP Calibration**
213 Previous CLAMP analyses of Late Cretaceous Arctic leaves have been based on modern
214 gridded climate observations recorded between 1961 and 1990 at a spatial resolution of 0.5 x
215 0.5° (New, Hulme & Jones 1999), with interpolations and altitude corrections to the exact
216 location of the vegetation stands comprising the CLAMP training sets

(https://www.paleo.bristol.ac.uk/ummodel/scripts/html_bridge/clamp_UEA.html). This calibration dataset is known as GridMet_3br (http://clamp.ibcas.ac.cn). Higher spatial resolution data are also available using the same observational network of meteorological stations. One such dataset is that of WorldClim2 (http://worldclim.org/version2) (Fick & Hijmans 2017), which interpolates average meteorological observations between 1970 and 2000 on to a spatial grid approximating to 1 km^2.

One advantage of using WorldClim2 for calibration is that numerous environmental variables have been mapped on to the same grid, so by using CLAMP the range of environmental signals decoded from leaf form can be extended. The new temperature-related environmental variables that correlate strongly with leaf form are 1) the compensated thermicity index (THERM.), 2) growing degree days above 0 °C (GDD_0), 3) growing degree days above 5 °C (GDD_5), 4) minimum temperature of the warmest month (MIN_T_W) and 5) maximum temperature of the coldest month (MAX_T_C). New humidity-related variables are 6) mean annual vapour pressure deficit (VPD.ANN), 7) mean summer vapour pressure deficit (VPD.SUN), 8) mean winter vapour pressure deficit (VPD.WIN), 9) mean spring vapour pressure deficit (VPD.SPR), 10) mean autumn vapour pressure deficit (VPD.AUT), 11) mean annual potential evapotranspiration (PET.ANN), 12) potential evapotranspiration during the warmest month (PET.WARM),13) potential evapotranspiration during the coldest month (PET.COLD), 14) soil moisture capacity (SOIL.M) and 15) the number of months when the mean temperature is above 10 °C. This last metric serves as a further comparison between the WorldClim2 data and previous calibrations because it should return values similar to those indicating the length of the growing season (LGS). For easy reference Table 1 summarises all the CLAMP metrics presented here.

Figures 6–10, graphs A–Z, illustrate the CLAMP regression models for each of the climate variables to show not only the relative position on the regression of the NPR fossil locations but also the scatter of the modern training data and thus the precision of the CLAMP predictions. All regression models are derived from the leaf physiognomy/climate relationships in 4D space as used in earlier CLAMP analyses (Herman & Spicer 1996b; 1997a; Spicer & Herman, 2010).

Formatted: Not Highlight

Deleted: Figure 5, parts a–e, illustrates the CLAMP regression models for each of the climate variables (Fig. 5, graphs A–Z) to show not only the relative position on the regression of the NPR fossil locations but also the scatter of the modern training data and thus the precision of the CLAMP predictions. All regression models are derived from the leaf physiognomy/climate relationships in 4D space as used in earlier CLAMP analyses (Herman &Spicer 1996b; 1997a; Spicer and Herman, 2010).¶

Formatted: Highlight

2.b. Climate Variable Definitions

Descriptions and regression models for the 11 standard CLAMP climate variables (mean annual temperature - MAT, warm month mean temperature - WMMT, cold month mean temperature - CMMT, length of the growing season - LGS, growing season precipitation - GSP, mean monthly growing season precipitation - MMGSP, precipitation during the three consecutive wettest months - 3WET, precipitation during the three consecutive driest months – 3DRY, mean annual relative humidity – RH. ANN, mean annual specific humidity – SH.ANN and mean annual moist enthalpy – ENTH) are given in the CLAMP website (http://clamp.ibcas.ac.cn) and summarised in Table 1. Here we describe the newly added climate variables.

The compensated thermicity index (THERM.) is given by

$$\text{THERM.} = ((T + m + M)*10) \pm C \quad (1)$$

where T is the mean annual temperature, m is the minimum temperature of the coldest month, M is the maximum temperature of the coldest month and C is a 'compensation value'. Calculating C is complicated and depends on continentality, which is simply a measure of the difference between the WMMT and the CMMT. In the extratropical zones of the World (northern and southern 27º parallels, respectively) THERM. is designed to equilibrate the large differences in temperature that occur between winter cold and summer warmth in

275 continental climates compared to those small differences that occur in maritime climates.
276 Details of how C is calculated are given in the Worldwide Bioclimatic Classification System
277 (www.globalbioclimatics.org) (Rivas-Martinez, Sanchez-Mata & Costa 1999).

278 GDD_0 is a measure of the cumulative heat available to plants and is the sum of the
279 mean monthly temperatures for months with mean temperatures greater than 0 °C multiplied
280 by number of days above that temperature.

281 GDD_5 is the sum of mean monthly temperatures for months with mean temperature
282 greater than 5 °C multiplied by number of days above that temperature.

283 VPD reflects the ease of losing water to the atmosphere and as such affects
284 transpiration as well as evaporation. It is the difference between the actual water vapour
285 pressure and the water vapour pressure at saturation. At saturation (VPD=0 kPa) water will
286 condense out to form clouds, dew or films of water on surfaces, including leaves. VPD
287 combines temperature and relative humidity so, unlike relative humidity, vapour-pressure
288 deficit has a simple nearly straight-line relationship to the rate of evapo-transpiration and
289 other measures of evaporation. Because of this, plant distribution (Huffaker 1942) and leaf
290 physiognomy are more strongly reflective of VPD.ANN than RH. ANN (Fig. 7, L, J). This
291 suggests strong leaf trait adaptations to overcoming transpiration depression at low VPDs.
292 Also, VPD is strongly correlated with stomatal conductance and carbon isotope fractionation
293 (e.g. Oren et al. 1999; Bowling et al. 2002; Katul, Palmroth & Oren 2009). As well as annual
294 mean VPD (VPD.ANN), seasonal VPD estimates (spring – VPD.SPR, summer – VPD.SUM,
295 autumn – VPD. AUT and winter – VPD.WIN) are also given by CLAMP.

296 Potential evapotranspiration (PET) is an expression of the ability of the atmosphere to
297 remove water through evapotranspirational processes assuming no limits on plant water
298 supply. Such an assumption appears valid in the case of the early Late Cretaceous Arctic as
299 evidenced by the widespread occurrence of thick coals indicative of raised mires (Sable &

Deleted: 5b
Deleted: I
Deleted: J

Stricker 1987; Grant, Spicer & Parrish 1988), gleyed palaeosols and isotopic analysis (Ufnar et al. 2004). PET combines the energy available for evaporation and the capacity of the lower atmosphere to move evaporated water vapour away from the land surface, for example by winds and convective processes. Because solar radiation provides the energy for evaporation, PET is lower on cloudy days, in winter and at higher latitudes. Like VPD, PET can be thought of as an indication of how difficult it is for a plant to transpire, a process that is essential for moving water and nutrients from the soil to the leaves. Because of this, and as with VPD, leaf physiognomy correlates well with PET (Fig. 8, Q; Fig. 9, V & W) particularly at low PET values. Although herbaceous plants transpire less than woody plants because they have a lower leaf surface area, the PET reference measure is based on uniformly short grass completely covering the ground. PET estimates for the warmest month (PET.WARM, Fig. 9, V) and coldest month (PET.COLD, Fig. 9, W) are given as well as the mean annual PET (PET.ANN, Fig. 8, Q).

In the work presented here we introduce a new CLAMP calibration based on WorldClim2 that we call WorldClim2_3br. As well as using the WorldClim2 gridded climate data for the standard CLAMP climate variables, we add the 15 new climate variables considered above. The new WorldClim2-based climate training set (WorldClim2_3br) and the accompanying modern leaf physiognomic (Physg3brcAZ) data files are given in the *Supplementary Materials*.

2.c. Fossil Assemblages

Here we re-analyse eight well-documented fossil leaf assemblages (see http://arcticfossils.nsii.org.cn) from across the NPR (Figs. 1 & 2) spanning the Cenomanian to Coniacian. All have been previously analysed for the standard CLAMP climate variables

Deleted: 5
Deleted: c
Deleted: –S
Deleted: 5c
Deleted: R
Deleted: 5c
Deleted: S
Deleted: 5
Deleted: c
Deleted: WorldClim3

calibrated using low spatial resolution modern gridded climate data (GridMet_3br) (Spicer & Herman 2010; Herman, Spicer & Spicer 2016). We use the same modern vegetation trait scores as used previously (Physg3brcAZ) but with the new WorldClim2_3br ~1 km^2 gridded data and with 15 new environmental variables. Where palaeolatitudes are quoted they are derived from GeTech.Plc palaeogeographies (an example of which is shown in Fig. 2) used in climate modelling (http://www.bridge.bris.ac.uk/resources/simulations). These palaeogeographies time-integrate a range of geological data and include plate kinematics. CLAMP scoresheets for these fossil assemblages are given in the *Supplementary Materials*.

3. Results and Discussion

Tables 2–4 present results obtained for the fossil assemblages using the new WorldClim2_3br CLAMP calibration as well as (for comparison) previously obtained results that used low spatial resolution GridMet_3br CLAMP calibration. The GridMet_3br results are given in parentheses. Figures 6–10, graphs A–Z, show the CLAMP regression models for the new WorldClim2_3br calibration and the positions of the fossil sites on the regression model. The regression models indicate the relationship between leaf physiognomy and the individual climate variable and thus the precision of the predictions. They also indicate the positions of the values for each fossil assemblage for each climate variable relative to those for modern vegetation. Note that despite essentially the same observational network of meteorological stations underpinning both gridded datasets, GridMet_3br and WorldClim2_3br calibrations rarely yield identical results. These differences are purely a function of the different gridding processes between the GridMet_3br and WorldClim2_3brc and a slightly different period of climate observations: 1961–1990 in the case of GRIDMet_3br and 1970–2000 for WorldClim2_3br. Such differences define the maximum predictive precision possible for any

Deleted: 1
Deleted: 3
Deleted: 5a-e

proxy using modern gridded climate observations for calibration because they are a measure of how well we can quantify modern climate.

3.a. Thermal regime

While not identical, the two calibrations yield similar results regarding the thermal regime and the differences are smaller than, or the same as, the uncertainties. They show clearly that despite the lack of winter insolation terrestrial CMMTs across the Arctic NPR region, even at latitudes as high as ~80 °N, rarely fell below freezing. This might appear surprising for the highest palaeolatitudes (Novaya Sibir – 81.6 °N, North Slope Alaska – 77 °N) that experienced more than three months of continuous winter darkness (Fig. 3), but these sites were close to the Arctic Ocean coastline and several lines of evidence point to the Arctic Ocean being warm with winter sea surface temperatures of ~6 °C (Herman & Spicer 1997a), or even approaching 10 °C as indicated here by the winter coastal plain temperatures of the North Slope, Alaska.

[Table 2 near here]

The estimates for the length of the growing season are also consistent with the light regimes at different palaeolatitudes (Figs. 3–5). Because leaf load is directly related to transpiration and the humidity regime, we have attempted to estimate the timing of bud break and leaf fall in the predominantly deciduous NPR vegetation. Bud break and leaf fall likely occurred in early March and late October respectively in the Cenomanian Vilui Basin (palaeolatitude 72 °N, LGS 7.5 months) when mean temperatures rose above 10 °C and there was at least 8 hours of direct sunlight (Fig. 5).

Deleted: 2

Deleted: 1

Deleted: 2

Deleted: 4

Deleted: 4

[Figure 3 near here]

In Grebenka, also Cenomanian but at 74 °N, the growing season is similar with a slightly warmer winter despite the slightly higher latitude (Fig. 4). The Penzhina assemblage (Plat. 72 °N) has a shorter growing season of around 5 months due to the lower winter temperature (Fig. 5). The 10 °C mark was not passed until almost mid-April when there were 16 hours of direct sunlight during each 24-hour period and the growing season lasted until late September when temperatures dipped below 10 °C and daylight hours approached 12. The foliage traits of the highest palaeolatitude assemblage, Novaya Sibir (Turonian, Plat. ~82 °N), suggest that bud break occurred in early April and growth continued until the beginning of October, a growing period of 5.8 months. The Coniacian North Slope assemblage from the northern Alaska palaeo-floodplain has the longest growing season (7.5 months) despite its palaeolatitude of ~78 °N. This is because winter temperatures barely dipped below 10 °C (Table 2, Fig. 3) and although the mean air temperature would have passed 10 °C in mid February and dipped below 10 °C in early November, a period of ~8.5 months, growth must have been moderated by insolation. With relatively warm conditions maintained by a nearby warm Arctic Ocean we estimate that a minimum of 4 hours of direct sunlight per 24-hour period is likely to have been the critical driver for leaf expansion and abscission, meaning that bud burst likely took place in late February and leaf fall in early-mid October. Early Late Cretaceous North Slope tree ring characteristics (Parrish & Spicer 1988a) indicate the rapid onset of growth and a prolonged and uninterrupted summer growth period.

3.b. Relative Palaeoelevations

The differences in thermal regime between the various leaf fossil assemblages used in our analyses depend not only on their palaeo-position but also on their relative elevations above

Deleted: 2
Deleted: 3
Deleted: 4
Deleted: 1
Deleted: 2
Deleted: ¶

sea level. Clues to these elevational differences come from the moist enthalpy estimates (Table 3). The North Slope assemblage is known to represent near sea level conditions because the plant-bearing units inter-finger with marine sediments (Mull, Houseknecht & Bird 2003), and as would be expected this site yields the highest moist enthalpy value indicative of the lowest elevation. The site with the lowest moist enthalpy value (highest elevation) is in the Okhotsk-Chukotka Volcanogenic Belt (Arman) and the difference between the two enthalpy values is 20 kJ/kg (Table 3) which translates to a height difference of ~2 km (Forest, Molnar & Emanuel 1995; Spicer 2018). However, this difference is not spatially or temporally corrected. The Arman site has been estimated to have been at ~0.6 km using the Kaivayam assemblage as a sea level datum and the GridMet_3br calibration (Herman 2018). Using the new WorldClim2_3brc raises this surface height estimate for the Arman flora to ~0.9 ± 0.8 km. Based on the relative palaeo-enthalpy estimates all the NPR localities likely were below 1 km elevation, but detailed analysis awaits future moist enthalpy fields derived from integrating proxy and palaeoclimate modelling.

[Figure 4 near here]

[Figure 5 near here]

3.c. Precipitation

Table 3 shows the estimated precipitation regime derived from leaf form. In general, the wetter the climate the less well leaf physiognomy predicts the precipitation regime (Figs. 6 & 7, E-H). Many of the Arctic angiosperm leaves are large (Herman 1994), which is an advantageous adaptation to low and predominantly diffuse sunlight situations provided that water is abundant. Abundant thick Late Cretaceous coals (Sable & Stricker 1987), many of

Deleted: 2
Deleted: 2
Deleted: 3
Deleted: 4
Deleted: 2
Deleted: 5a
Deleted: ,
Deleted: b

458 which represent raised mires (Youtcheff, Rao & Smith 1987; Grant, Spicer & Parrish 1988),
459 and isotope analyses (Ufnar et al. 2004) all suggest that early Late Cretaceous Arctic annual
460 precipitation was high.
461
462 [Table 3 near here]
463
464 Although we can be certain that in general the Late Cretaceous Arctic was wet,
465 deriving accurate precipitation estimates from high latitude palaeofloras is problematic for
466 several reasons. Firstly, leaf fossils are invariably preserved in aquatic environments where
467 low oxygen limits decay. The limited distance that leaves can be transported from their
468 growth site before burial (Spicer 1981; Ferguson 1985; Spicer & Wolfe 1987) means that the
469 source plants most likely grew in locations where the water table was high year-round. The
470 estimate of soil moisture capacity for the NPR fossil assemblages (Table, 3 SOIL_M, Fig. 9,
471 U) also suggests moist soils. Moreover, this water may not reflect local precipitation but
472 conditions in the headwaters of the river catchment many tens if not hundreds of kilometres
473 away. Secondly, even if the water table was maintained by local precipitation, the soil system
474 stores water and buffers seasonal variations in water availability, meaning that 3WET and
475 3DRY estimates represent seasonality in rainfall only poorly. Thirdly, at high latitudes where
476 light and temperature impose dormancy and seasonal leaf-shedding, rainfall in the dormant
477 period is unlikely to be reflected in leaf physiognomy. This is not the case, however, for
478 winter temperatures.
479 Winter temperatures are to some extent encoded in leaf physiognomy (Fig. 6, C)
480 because young leaves have to be adapted to rapidly warming spring conditions, the rate of
481 warming being determined in large part by the CMMT (Spicer, Herman & Kennedy 2004).
482 However, below observed winter temperatures of -10 °C this extrapolative encoding, which

Deleted: 2
Deleted: 2
Deleted: 5d
Deleted: 5a

tends to yield winter temperatures that are too warm (Spicer, Herman & Kennedy 2004), does not apply at all to winter precipitation where soil moisture may be high year-round but inaccessible to the plant in early spring if the soil is frozen. The GSP estimate (note not the mean annual precipitation) of between 50 and 125 cm is quite low where the regression model shows little scatter (Fig. 6, E), but because the growing season is often less than half the year this indicates that overall the annual precipitation could have been at least double that indicated. Although CLAMP routinely returns estimates for precipitation during the three wettest (3WET) and three driest months (3DRY), these values may be unreliable because of the marked growth seasonality. In view of the arguments just given for wet soils it is noteworthy that there is a marked difference in the 3WET:3DRY ratio, which for all assemblages except Vilui B return ratios near 4:1.

Deleted: 5a

Deleted: ¶
[Figure 5 a near here]¶
¶
[Figure 5 b near here]¶
¶
[Figure 5 c near here]¶

The wet soils would necessarily mute these ratios, so the fact that they are pronounced suggests even more extreme rainfall seasonality than the values suggest and that the Arctic may have experienced a 'monsoonal' climate in the early Late Cretaceous. An essentially 'summer wet' (wet:dry ratio 3:1) has been proposed for the Arctic in the Eocene based on isotopic analysis of fossil wood interpreted to have been evergreen (Schubert et al. 2012), but an 'ever wet' precipitation regime for this Epoch is indicated by leaf form (West, Greenwood & Basinger 2015) based on predominantly deciduous angiosperm taxa. To really understand the hydrological regime in a warm Arctic requires, as far as is possible, decoupling the soil water environment from that of the atmosphere.

3.d. Humidity

Until now CLAMP has routinely returned only two humidity measures: mean annual relative humidity (RH.ANN) and mean annual specific humidity (SH.ANN). SH is simply the amount

of water in grams contained within a kilogram of dry air and as such is a measure of the absolute water content of the air. Leaf form appears to code for mean annual SH quite well in that the CLAMP regression model (Fig. 7, J) shows relatively little scatter compared to that of mean annual RH (Fig. 7, I). RH is a measure of the amount of water in the atmosphere relative to what it can hold and as such is highly dependent upon temperature. As the scatter in Fig. 7, I shows leaf form does not correlate well with RH so CLAMP predictions of RH carry a lot of uncertainty.

A better measure of humidity, one that reflects the force opposing transpiration, is vapour pressure deficit (VPD). VPD is the difference between the amount of moisture actually in the air and how much moisture the air could potentially hold when it is saturated and, like SH, is not measured in relation to temperature. High VPD values are found in arid environments while low VPDs reflect air close to saturation and thus a high resistance to transpiration.

Figs. 7 & 8, L-P, show that at low VPD values leaf form correlates very well with VPD, presumably because leaves have to possess adaptations to enhance transpiration, while in high VPD situations transpiration can take place easily without the need for specific leaf trait spectra to increase transpiration. Thus, there is more scatter in the CLAMP regressions at high VPDs. So, unlike precipitation, CLAMP estimates of VPD in moist regimes are generally more precise than in dry regimes.

[Table 4 near here]

Table 4 shows that all the Arctic early Late Cretaceous leaf assemblages indicate low VPDs (<5 kPa) in spring, autumn and winter but, because autumn and winter are times when leaves are senescent or shed, these values have to be interpreted with caution. The spring and

Deleted: 5b

Deleted: 5b

Deleted: 5b

Deleted: ¶
[Figure 5 d near here]¶

Deleted: [Figure 5 e near here]¶

Deleted: 5b

Deleted: and

Deleted: c

Deleted: 3

Deleted: 3

summer values are likely to be the most reliable because this is when the leaves are functional. The highest summer VPDs are those from fossil assemblages in NE Russia (Grebenka, Arman, Tylpegyrgynai) and these assemblages also point to the lowest annual RH values, while the lowest summer VPD and annual values are revealed in assemblages from the Arctic Ocean coastal areas (Novaya Sibir, North Slope), the Yukon-Koyukuk Basin and the Vilui Basin. These assemblages also indicate the highest RH.ANN values. Of all the Arctic fossil sites those bordering the Arctic Ocean and nearest the palaeo-pole (Novaya Sibir and North Slope) have the lowest VPDs, the only exception being the North Slope that has a VPD.WIN value similar to those of Grebenka and Arman. These assemblages also indicate the warmest winter temperatures (Fig. 3). However, even assemblages indicating the driest summers have very low VPDs compared to most modern vegetation in the calibration (Figs. 7 & 8, L–P), indicating an overall extremely wet atmosphere compared to that experienced by most vegetation in the modern CLAMP training sets.

PET is a measure of how easily the atmosphere removes water from a surface and so, like VPD, indicates the ease with which transpiration can take place. Also, like VPD, PET shows a close relationship with leaf trait spectra at low PET values i.e. wet regimes. All NPR fossil assemblages fall in the lower half of the regressions showing that they experienced similar PETs as modern vegetation in the more humid half of the 3br training set. The PET.WARM and PET.COLD values also show that any dry season was in the summer, presumably because higher temperatures and convective winds favoured greater evaporation.

Taking Figures 3–5 together it is noticeable that Figure 4 shows the highest humidities and that these occur at palaeolatitude ~75 °N from sites (Grebenka and Tylpegyrgynai) that were not immediately adjacent to the Arctic Ocean, but closer to the north Pacific. These high humidities may be a function of a cool northern Pacific gyre

Deleted: 5
Deleted: c
Deleted: 5 b
Deleted: and
Deleted: c
Deleted: 2
Deleted: 4
Deleted: 3

(Herman & Spicer 1996a, 1997a) or reflect a more northward and diffuse palaeoposition of the polar front, which today is located at ~60 °N as a consequence of a strong polar high.

4. Conclusions

4.a. Thermal regime.

The new WorldClim2_3br CLAMP calibration confirms earlier isotopic (Amiot et al. 2004), vegetation (Parrish & Spicer 1988b) and leaf physiognomic analyses (Herman & Spicer 1996b, 1997a; Spicer & Herman 2010) from the NPR demonstrating a thermal regime that may be broadly characterised as 'temperate' even at palaeolatitudes as high as ~80 °N where freezing temperatures were of limited duration and severity. The precision of the palaeoclimate regime estimates are constrained by the uncertainties associated with our inability to quantify precisely modern climate. These uncertainties, which will differ between calibration suites depending on calibration sampling distribution, density and temporal coverage, apply to any palaeoenvironmental proxy that relies on calibrations using the modern conditions and should not be ignored when making inter-proxy comparisons or interpreting past environments. In the analyses presented here MAT estimates differ by up to 0.6 °C, WMMT by up to 0.9 °C and CMMT by up to 1.5 °C depending purely on the underlying modern gridded climate data.

Deleted: and

Deleted: and

Deleted: and

Deleted: region

4.b. Palaeoelevation

No terrestrial palaeotemperature comparisons can be meaningful without taking into account differences in the surface height at which the estimates are made. In the case of the early Late Cretaceous NPR it is clear that some thermal differences between assemblages can be attributed to relative elevational differences, but that no site was likely to have been above 1 km. However, a 1 km elevation range can translate into MAT differences of several

degrees Celsius depending on early Late Cretaceous near polar terrestrial lapse rates. This aspect of the NPR palaeoclimate, and better characterisation of Late Cretaceous moist enthalpy fields, await future modelling work.

4.c. Precipitation and humidity

The precipitation regime throughout the NPR overall appears moderately wet with most sites indicating summer (growing season) precipitation ~0.5 m, but apparently with marked seasonal variations. Compared to all the sites in the modern calibration data humidity is high year-round, but with most evaporative stress occurring in the summer. PET (Table 4) never exceeds rainfall even in the summer growth period (Table 3), leading to year-round saturated soils. Drought was not limiting to growth in any of the NPR early Late Cretaceous localities and CMMTs (Table 2) were never low enough for long enough to freeze the soil to below tree rooting depth.

Our new insights into annual and seasonal atmospheric humidity in the warm early Late Cretaceous Arctic supports the concept of a very humid near-polar regime markedly different from today's frigid desert under a strong polar high-pressure cell and with a corresponding strong polar front at ~60 °N. It is likely that the polar front in the early Late Cretaceous was displaced towards the pole and more diffuse than at present. A key component of the weaker polar high was the warm Arctic Ocean that, as evidenced by year-round high humidities, generated a vigorous hydrological cycle, which in turn helped maintain the polar warmth.

The vegetation and climate records entombed in the extensive Late Cretaceous sediments of the Artic point towards what the North polar region is likely to experience as overall anthropogenic global warming progresses. Polar amplification will rapidly drive the Arctic from a place where at present precipitation is sparse under a cold strong polar high-

Deleted: region

Deleted: 3

Deleted: 2

Deleted: 1

Deleted:

pressure system to a region that is wet and polar air masses become increasingly loosely constrained as warming proceeds and the polar high weakens. The hydrological cycle is likely to become invigorated through warming-induced evaporation and enhanced transpiration from greater vegetation cover and complexity. Eventually this will result in a near permanent polar cloud cap, high humidity and frequent fog occurrences over both land and sea, further enhancing warming.

Acknowledgements. The research was performed within the framework of the State program no. 0135-2019-0044 of the Geological Inst., Russian Acad. Sci. and partly supported by the Russian Foundation for Basic Research project no. 19-05-00121 (AH). CLAMP recalibration was made possible through NSFC-NERC joint research program (41661134049 and NE/P013805/1) (PJV) and an XTBG International Fellowship for Visiting Scientists (RAS).

Declarations of Interest

All authors declare no competing interests.

Online Supplementary Material at http://journals.cambridge.org/geo

References

ALEKSEEV, P.I., HERMAN, A.B. & SHCHEPETOV, S.V. 2014. New angiosperm genera from Cretaceous sections of Northern Asia. *Stratigraphy and Geol. Correlation*, **22**(6), 606–617.

AMIOT, R., LECUYER, C., BEUFFETAUT, E., F., F., LEGENDRE, S. & MEARTINEAU, F. 2004. Latitudinal temperature gradient during the Cretaceous Upper-Campanian-Middle Maastrichtian: ∂O18 record of continental vertebrates. *Earth and Planetary Science Letters*, **226**, 255–272.

Deleted: 2016

Deleted: 0001

Commented [RAS1]: Alexei - what other works should go in here? It would be good to add more recent Russian ones.

Formatted: Indent: Left: 0 cm, Hanging: 1 cm, Line spacing: single

Deleted: -

675 BOWLING, D.R., MCDOWELL, N.G., BOND, B.J., LAW, B.E. & EHLERINGER, J.R. 2002. ^{13}C
676 content of ecosystem respiration is linked to precipitation and vapor pressure deficit.
677 *Oecologia*, **131**, 113–124.
678 BUDANTSEV, L.Y. 1968. Late Cretaceous flora of the Vilui Depression. *Botanicheskii*
679 *Zhurnal*, **53**, 3–16.
680 BUDANTSEV, L.Y. 1983. *Istoriya Arkticheskoi Flory Epokhi Rannego Kainofita (Arctic Flora*
681 *History in the Early Cenophytic Epoch)*. Nauka, Leningrad.
682 CRAGGS, H.J. 2005. Late Cretaceous climate signal of the Northern Pekulney Range Flora of
683 northeastern Russia. *Palaeogeography, Palaeoclimatology, Palaeoecology*, **217**, 25–46.
684 DECKER, P.L., WILSON, G.C., WATTS, A.B. & WORK, D. 1997. Growth position petrified trees
685 over-lying thick Nanushuk Group coal, Lili Creek, Lookout Ridge Quadrangle, North
686 Slope Alaska. *In*: Clough, J.G. & Larson, F. (eds) *Short Notes on Alaskan Geology*
687 *1997*. Alaska Division of Geological and Geophysical Surveys, 63–70.
688 DETTERMAN, R.L. & SPICER, R.A. 1981. New stratigraphic assignment for rocks along
689 Igilatvik (Sabbath) Creek, William O. Douglas Wildlife Range, Alaska. U.S.
690 Geological Survey in Alaska, accomplishments during 1979. *U.S. Geological Survey*
691 *Circular*, **823-B**, 11–12.
692 FERGUSON, D.K. 1985. The origin of leaf-assemblages - new light on an old problem. *Review*
693 *of Palaeobotany and Palynology*, **46**, 117–188.
694 FICK, S.E. & HIJMANS, R.J. 2017. Worldclim2: New 1-km spatial resolution climate surfaces
695 for global land surfaces. *International Journal of Climatology*, **37**, 4302–4315,
696 http://doi.org/https://doi.org/10.1002/joc.5086.
697 FILIPPOVA, G.G. 1975a. Flora of the Lower Cretaceous deposits of the Umkuveem and
698 Ainakhkurgen Depressions. *Materialy po geologii i poleznym iskopayemym Severo-*
699 *Vostoka SSSR*, **22**, 23–35.

Deleted: -

Deleted: -

Deleted: -

Deleted: -

FILIPPOVA, G.G. 1975b. On the age of the volcanogenic deposits of the left bank of the Palyavaam River (Chukotka). *Proceedings of the Institute of Biology and Pedology, Far Eastern Scientific Centre, USSR Academy of Sciences, New Series [Trudy Biologo-Pochvennogo Instituta DVNTs AN SSSR, Novaya Seriya]*, **27**, 55–59.

FILIPPOVA, G.G. 1979. Cenomanian flora of the Grebenka River and its stratigraphic significance *Dalnevostochnaya Paleofloristika (Palaeofloristics of the Far East)*. Trudy Biologo-Pochvennogo Instituta DVNTs Academii Nauk SSSR, Novaya Seriya, **53**, 91–115.

FILIPPOVA, G.G. 1988. Grebenka floristic assemblage in the Anadyr River basin (Chukotka). *Tikhookeanskaya Geologiya*, **17**, 50–60.

FILIPPOVA, G.G. 1989. New data on the Grebenka Flora from the Anadyr River Basin *Vulkanogennyi Mel Dalnego Vostoka (Volcanogenic Cretaceous of the Far East)*. DVO Academii Nauk SSSR, Vladivostok, 76–87.

FILIPPOVA, G.G. 1994. Coniacian flora of the northern part of the Pekulnei Range. *Kolyma*, March 1994, 13–21.

FILIPPOVA, G.G. & ABRAMOVA, L.N. 1993. *Late Cretaceous flora of North-eastern Russia.* Nedra, Moscow.

FOREST, C.E., MOLNAR, P. & EMANUEL, K.E. 1995. Palaeoaltimetry from energy conservation principles. *Nature*, **343**, 249–253.

FREDERIKSEN, N.O., AGER, T.A. & EDWARDS, L.E. 1988. Palynology of Maastrichtian and Paleocene rocks, lower Colville River region, North Slope of Alaska. *Canadian Journal of Earth Sciences*, **25**, 512–527.

GOLOVNEVA, L.B. 1988. Novyi rod *Microconium* (Cupressaceae) iz pozdnemelovykh otlozhenii Severo-Vostoka SSSR (A new genus *Microconium* (Cupressaceae) form the

Deleted: -

Deleted: -

Deleted: -

Formatted: Font: Not Bold

Deleted: -

Formatted: Font: Not Bold

Deleted: -

Formatted: Font: Not Bold

Deleted: -

Late Cretaceous deposits of the North-East of the USSR). *Botanicheskii Zhurnal*, **73(8)**, 1179–1184 (in Russian).

GOLOVNEVA, L.B. 1991a. Novyi rod *Palaeotrapa* (Trapaceae?) i novye vidy *Quereuxia* iz rarytkinskoi svity (Koryakskoye nagor'ye, maastrikht-danii (The new genus *Palaeotrapa* (Trapaceae?) and new species *Quereuxia* from the Rarytkin Formation (the Koryak Upland, Maastrichtian - Danian)). *Botanicheskii Zhurnal*, **76(4)**, 601–610 (in Russian).

GOLOVNEVA, L.B. 1991b. Vidy roda *Trochodendroides* (Cercidiphyllaceae) v maastrikht-datskoi rarytkinskoi flore Koryakskogo nagor'ya (The species of the genus *Trochodendroides* (Cercidiphyllaceae) in Maastrichtian - Danian Rarytkin Flora of the Koryak Upland). *Botanicheskii Zhurnal*, **76(3)**, 427–436 (in Russian).

GOLOVNEVA, L.B. 1994a. Maastrichtian–Danian Floras of Koryak Uplands. *Trudy Botanicheskogo Instituta, VL Komarova*, **13**, 1–145.

GOLOVNEVA, L.B. 1994b. The flora of the Maastrichtian–Danian deposits of the Koryak Uplands, northeast Russia. *Cretaceous Research*, **15**, 89–100.

GOLOVNEVA, L.B. 2000. The Maastrichtian (Late Cretaceous) climate in the Northern Hemisphere. *In*: Hart, M.B. (ed) *Climates: past and present*. Geological Society of London Special Publication, London, **181**, 43–54.

GOLOVNEVA, L.B., & ALEKSEEV, P. I. 2010. The genus *Trochodendroides* Berry in the Cretaceous floras of Siberia. In: Budantsev, L.Yu. (ed.), *Palaeobotany*, Vol. **1**, 120–166 [in Russian, English summary].

GOLOVNEVA, L.B. & HERMAN, A.B. 1992. New data on composition and age of flora of the Koryak Formation (Borth-eastern Russia). *Botanicheskii Zhurnal*, **77(7)**, 60–71.

Deleted: -
Deleted: -
Deleted: -
Deleted: -
Deleted: -
Deleted: -
Formatted: Small caps
Formatted: Line spacing: Double
Formatted: Font: Bold
Formatted: Check spelling and grammar
Formatted: Normal, Line spacing: single
Deleted: -

765 GOLOVNEVA, L.B., HERMAN, A.B., & SHCZEPETOV, S.V. 2015. The genus *Menispermites*
766 Lesquereux (angiosperms) in the Cretaceous Grebenka Flora of Northeastern Russia.
767 *Paleontological Journal*, **49**(4), 429–437.
768 GOLOVNEVA, L.B. & SHCHEPETOV, S.V. 2015. Floristic assemblages from Upper Cretaceous
769 deposits of East Chukotka. In: *Paleobotanika (Palaeobotany)*, Vol. **6**. St. Marafon,
770 Petersbourg, 96–119 [in Russian].
771 GOLOVNEVA, L.B., SHCHEPETOV, S.V., & ALEKSEEV, P.I. 2011. Chingandzha Flora (Late
772 Cretaceous, North-eastern Russia): systematic composition, palaeoecological features
773 and stratigraphic significance. In: *Lectures in Memory of A.N. Kryshtofovich*, Iss. **7**, 37–
774 61 [in Russian].
775 GRANT, P.R., SPICER, R.A. & PARRISH, J.T. 1988. Palynofacies of northern Alaskan
776 Cretaceous coals. *7th International Palynological Congress Brisbane, Abstracts*
777 *Volume*, **60**.
778 HERMAN, A.B. 1990. Late Cretaceous Floras and Climate of the Anadyr-Koryakian
779 Subregion (North-East USSR). *Proceedings of the Symposium "Paleofloristic and*
780 *Paleoclimatic Changes in the Cretaceous and Tertiary*, 73–79.
781 HERMAN, A.B. 1991. Cretaceous angiosperms and phytostratigraphy of North-Western
782 Kamchatka and Yelistratov Peninsula. *In*: Herman, A.B. & Lebedev, E.L. (eds)
783 *Stratigraphy and flora of the Cretaceous of north-western Kamchatka*. Nauka,
784 Moscow, 5–141.
785 HERMAN, A.B. 1993. Late Maestrichtian flora from the Emima-ll'naivaam Interfluve, the
786 northeastern Koryak Highland, and its stratigraphic significance. *Stratigraphy and*
787 *Geological Correlation*, **1**, 427–434.

Formatted: Small caps
Formatted: Small caps
Formatted: Font: Bold
Formatted: Small caps
Formatted: Normal
Formatted: Font: Bold
Formatted: Check spelling and grammar
Formatted: Font: Bold
Deleted: -
Deleted: -
Deleted: -

HERMAN, A.B. 1994. Late Cretaceous Arctic platanoids and high latitude climate. *In*: Boulter, M.C. & Fisher, H.C. (eds) *Cenozoic Plants and Climates of the Arctic (NATO ASI Ser., I 27)*. Springer, Berlin, 151–159.

HERMAN, A.B. 2002. Late Early-Late Cretaceous floras of the North Pacific Region: florogenesis and early angiosperm invasion. *Review of Palaeobotany and Palynology*, **122**, 1–11.

HERMAN, A.B. 2007. Comparative paleofloristics of the Albian-early Paleocene in the Anadyr-Koryak and North Alaska Subregions, Part 1: The Anadyr-Koryak Subregion. *Stratigraphy and Geological Correlation*, **15**, 321–332.

HERMAN, A.B. 2011. *Al'bskaya – Paleotsenovaya Flora Severnoi Patsifiki (Albian – Paleocene Flora of the North Pacific Region)*. GEOS, Moscow.

HERMAN, A.B. 2013. Albian – Paleocene Flora of the North Pacific: Systematic Composition, Palaeofloristics and Phytostratigraphy. *Stratigraphy and Geological Correlation*, **21**(7), 689–747.

HERMAN, A.B. 2018. On the likely palaeoelevation of the Turonian-Coniacian Arman Flora site (North-Eastern Asia). *Fossil Imprint*, **74**, 159–164.

HERMAN, A.B., AKHMETIEV, M.A., KODRUL, T.M., MOISEEVA, M.G. & IAKOVLEVA, A.I. 2009. Flora Development in Northeastern Asia and Northern Alaska during the Cretaceous–Paleogene Transitional Epoch. *Stratigraphy and Geological Correlation*, **17**, 79–97.

HERMAN, A.B., GOLOVNEVA, L.B., SHCZEPETOV, S.V., & GRABOVSKY, A.A. 2016. The Late Cretaceous Arman Flora of Magadan Oblast, Northeastern Russia. *Stratigraphy and Geological Correlation*, **24**(7), 651–760.

Deleted: -

Deleted: -

Deleted: -

Formatted: Small caps

Formatted: Normal

Deleted: ¶

Deleted: -

Formatted: Small caps

Formatted: Small caps

HERMAN, A.B., KOSTYLEVA, V.V., NIKOLSKII, P.A., BASILYAN, A.E., & KOTEL'NIKOV, A.E. 2019. New data on the Late Cretaceous flora of the New Siberia Island, New Siberian Islands. *Stratigraphy and Geological Correlation*, **27**(3).

HERMAN, A.B. & LEBEDEV, Y.L. 1991. *Stratigraphy and flora of the Cretaceous deposits of North-West Kamchatka.* Academy of Sciences of the USSR Report **468**.

HERMAN, A.B. & SHCZEPETOV, S.V. 1991. The Mid-Cretaceous flora of the Anadyr river basin (Tchukotka, NE Siberia). *Proceedings of the Pan-European Palaeobotanical Conference*, **Palaeovegetational development in Europe**, 273–279.

HERMAN, A.B. & SPICER, R.A. 1995. Latest Cretaceous flora of northeastern Russia and the ''Terminal Cretaceous Event'' in the Arctic. *Paleontological Journal*, **29**, 22–25.

HERMAN, A.B. & SOKOLOVA, A.B. 2016. Late Cretaceous Kholokhovchan Flora of Northeastern Asia: Composition, age and fossil plant descriptions. *Cretaceous Research*, **59**, 249–271.

HERMAN, A.B. & SPICER, R.A. 1996a. Palaeobotanical evidence for a warm Cretaceous Arctic Ocean. *Nature*, **380**, 330–333.

HERMAN, A.B. & SPICER, R.A. 1996b. *Nilssoniocladus* in the Cretaceous Arctic: new species and biological insights. *Review of Palaeobotany and Palynology*, **92**, 229–243.

HERMAN, A.B. & SPICER, R.A. 1997a. New quantitative palaeoclimate data for the Late Cretaceous Arctic: evidence for a warm polar ocean. *Palaeogeography, Palaeoclimatology, Palaeoecology*, **128**, 227–251.

HERMAN, A.B. & SPICER, R.A. 1997b. The Koryak flora: did the early Tertiary deciduous flora begin in the late Maastrichtian of northeastern Russia? *Mededelingen Nederlands Instituuut voor Toegepaste Geowetenschappen TNO*, **58**, 87–92.

HERMAN, A.B., SPICER, R.A. & KVACEK, J. 2002. *In*: Wagreich, M. (ed) *Aspects of Cretaceous Stratigraphy and Palaeobiogeography. Proceedings 6th Internat.*

Formatted: Small caps
Formatted: Normal
Formatted: Font: Check spelling and grammar
Deleted: -
Deleted: -
Formatted: Small caps
Formatted: Font: Italic
Formatted: Font: Bold
Deleted: -
Deleted: -
Deleted: -

Cretaceous Symposium, Vienna 2000. Österreichische Academie der Wissenschaften, Schriftenreihe der Erdwissenschaftlichen Kommissionen, Vienna, **15**, 93–108.

HERMAN, A.B., SPICER, R.A. & SPICER, T.E.V. 2016. Environmental constraints on terrestrial vertebrate behaviour and reproduction in the high Arctic of the Late Cretaceous. *Palaeogeogr., Palaeoclimatol., Palaeoecol.*, **441**, 317–338.

HOLLICK, A. 1930. The Upper Cretaceous Floras of Alaska. *United States Geological Survey Professional Paper*, **159**, 1–123.

HUFFAKER, C.B. 1942. Vegetational Correlations with Vapour Pressure Deficit and Relative Humidity. *American Midland Naturalist*, **28**, 486–500.

IPCC (ed) 2014. *Synthesis Report. Contribution of Working Groups I, II and III to the Fifth Assessment Report of the Intergovernmental Panel on Climate Change. Core Writing Team.* IPCC, Geneva, Switzerland, 151.

KATUL, G.G., PALMROTH, S. & OREN, R. 2009. Leaf stomatal responses to vapour pressure deficit under current and CO2- enriched atmosphere explained by the economics of gas exchange. *Plant Cell Environment*, **32**, 968–979.

KIRITCHKOVA, A.I. & SAMYLINA, V.A. 1978. Korrelyatsiya nizhnemelovykh otlozhenii Lenskogo uglenosnogo basseina i Severo-Vostoka SSSR (Correlation of Lower Cretaceous deposits of Lena coal-bearing basin and North-eastern USSR). *Soviet Geol.*, **12**, 3–18.

KOVACH, W.L. & SPICER, R.A. 1996. Canonical correspondance analysis of leaf physiognomy: a contribution to the development of a new palaeoclimatological tool. *Palaeoclimates*, **2**, 125–138.

KRASSILOV, V.A. 1975. Climatic changes in Eastern Asia as indicated by fossil floras. II Late Cretaceous and Danian. *Palaeogeography, Palaeoclimatology, Palaeoecology*, **17**, 157–172.

Deleted: -

Deleted: s

Deleted: -

Deleted: -

Deleted: -

KRASSILOV, V.A. 1978. Late Cretaceous gymnosperms from Sakhalin, U.S.S.R., and the terminal Cretaceous event. *Palaeontology*, **21 (4)**, 893–905.

LEBEDEV, Y.L. 1965. Late Jurassic Flora of Zeia River and the Jurassic - Cretaceous Boundary. *Academy of Sciences of the USSR*, **125**, 5–142.

LEBEDEV, Y.L. 1976. Evolution of Albian-Cenomanian floras of Northeast USSR and the association between their composition and facies conditions. *International Geology Review*, **19**, 1183–1190.

LEBEDEV, Y.L. 1987. Stratigraphy and age of the Okhotsk-Chukotsk volcanogenic belt. *Academy of Sciences of the USSR*, **421**, 3–175.

LEBEDEV, Y.L. 1992. The Cretaceous floras of Northeastern Asia. *Izvestiya Akademii Nauk, seriya geologicheskaya*, **4**, 85–96.

LEBEDEV, Y.L. & HERMAN, A.B. 1989. A new genus of Cretaceous angiosperms- *Dalembia*. *Review of Palaeobotany and Palynology*, **59**, 77–91.

LEE, S. 2014. A theory for polar amplification from a general circulation perspective. *Asia-Pacific Journal of the Atmospheric Sciences*, **50**, 31–43.

LOTTES, A.L. 1987. Paleolatitude determinations: comparison of palaeoclimatic and palaeomagnetic methods. *Geological Society of America Abstracts with Program*, **19**, 749.

MULL. C.G., HOUSEKNECHT, D.W. & BIRD, K.J. 2003. Revised Cretaceous and Tertiary stratigraphic nomenclature in the Colville Basin, Northern Alaska. *U.S. Geological Survey Professional Paper*, **1673**, 1–51.

NEW, M., HULME, M. & JONES, P. 1999. Representing Twentieth-Century Space–Time Climate Variability. Part I: Development of a 1961–90 Mean Monthly Terrestrial Climatology. *Journal of Climate*, **12**, 829–856.

Deleted: -

Deleted: -

Deleted: -

Deleted: -

Deleted: -

Deleted: -

NIKITENKO, B.L., DEVYATOV, V.P., LEBEDEVA, N.K., BASOV, V.A., GORYACHEVA, A.A., PESTCHEVITSKAYA, E.B., & GLINSKIKH, L.A. 2017. Jurassic and Cretaceous stratigraphy of the New Siberian Archipelago (Laptev and East Siberian seas): facies zoning and lithostratigraphy. *Geologiya i Geofizika*, **58**(12), 1867–1885 (in Russian).

NIKITENKO, B.L., DEVYATOV, V.P., LEBEDEVA, N.K., BASOV, V.A., FURSENKO, E.A., GORYACHEVA, A.A., PESTCHEVITSKAYA, E.B., GLINSKIKH, L.A., & KHAFAEVA, S.N. 2018. Jurassic and Cretaceous biostratigraphy and organic matter geochemistry of the New Siberian Islands (Russian Arctic). *Geologiya i Geofizika*, **59**(2), 211–230 (in Russian).

OREN, R., SPERRY, J.S., KATUL, G.G., PATAKI, D.E., EWERS, B.E., PHILLIPS, N. & SCHÄFER, K.V.R. 1999. Survey and synthesis of intra- and interspecific variation in stomatal sensitivity to vapour pressure deficit. *Plant Cell Environment*, **22**, 1515–1526.

PARRISH, J.T. & SPICER, R.A. 1988a. Middle Cretaceous wood from the Nanushuk Group, Central North Slope, Alaska. *Palaeonotology*, **31**, 19–34.

PARRISH, J.T. & SPICER, R.A. 1988b. Late Cretaceous terrestrial vegetation: a near-polar temperature curve. *Geology*, **16**, 2–25.

PIGLIUCCI, M. 2003. Phenotypic integration: studying the ecology and evolution of complex phenotypes. *Ecology Letters*, **6**, 265–272.

RIVAS-MARTINEZ, S., SÁNCHEZ-MATA, D. & COSTA, M. 1999. *Itinera Geobotanica*, **12**, 3–316.

SABLE, E.G. & STRICKER, G.D. 1987. Coal in the National Petroleum Reserve in Alaska (NPRA): framework geology and resources. *In*: Taileur, I. & Weimer, P. (eds) *Alaskan North Slope Geology*. Society of Economic Paleontologists and Mineralogists, Pacific Section, Bakersfield, California, **1**, 195–215.

Formatted: Small caps

Formatted: Small caps

Formatted: Normal

SAMYLINA, V.A. 1963. Mesozoic flora Aldan. Academiya Nauk S.S.S.R., P*aleobotanica*, ser. 8, **4**, 59–139.

SAMYLINA, V.A. 1968. Early Cretaceous angiosperms of the Soviet Union based on leaf and fruit remains. *J. Linnaean Soc. (Botany)*, **61**, 207–218.

SAMYLINA, V.A. 1973. Correlation of Lower Cretaceous continental deposits of Northeast USSR based on palaeobotanical data. *Sovietskaya Geologiya*, **8**, 42–57.

SAMYLINA, V.A. 1974a. Florae Cretae Prioris Partium Boreali-orientalium URSS. *Academia Scientiarum URSS*, 3–54.

SAMYLINA, V.A. 1974b. *Early Cretaceous floras of Northeast USSR (problems of establishing Cenophytic floras) [Rannemelovye flory severo-vostoka SSSR. K probleme stanovleniya flor Kainofita]*. Nauka, Leningrad.

SAMYLINA, V.A. 1976. The Cretaceous flora of Omsukchan (Magadan district). Komarov Botanical Institute of the Academy of Sciences of the USSR.

SAMYLINA, V.A. 1988. *Arkagala stratoflora of northeastern Asia [Arkagalinskaya sratoflora severo-vostoka Azii]*. Nauka, Leningrad.

SAMYLINA, V.A. & SHCZEPETOV, S.V. 1991. Ginkgovyye i chekanovskievyye iz verkhnemelovykh otlozhenii Yeliseevskogo obnazheniiy na r. Grebyonka (pravoberezh'ye r. Anadyr') (The ginkgoaleans and czekanowskialeans from the Upper Cretaceous deposits of the Yeliseev outcrop on the Grebenka River (the right bank of the Anadyr River)). *Botanicheskii Zhurnal*, **76(7)**, 950–956 (in Russian).

SCHUBERT, B.A., JAHREN, A.H., EBERLE, J.J., STERNBERG, L.S.L. & EBERTH, D.A. 2012. A summertime rainy season in the Arctic forests of the Eocene. *Geology*, **40**, 523–526.

SCOTT, R.A. & SMILEY, C.J. 1979. Some Cretaceous megafossils and microfossils from the Nanushuk Group, northern Alaska: a preliminary report. *U.S. Geological Survey Circular*, **794**, 89–111.

Formatted: EndNote Bibliography

Formatted: Font: Palatino

Deleted: SAMYLINA, V.A. 1968. Early Cretaceous angiosperms of the Soviet Union based on leaf and fruit remains. *J. Linnaean Soc. (Botany)*, **61**, 207–218.¶

SHCZEPETOV, S.V. 1991. *Mid Cretaceous flora of the Chauna Group (central Chukotka): stratigraphic setting, systematic composition, atlas of plants [Srednemelovaya flora Chaunskoi Serii (tsentral'naya Chukotka): stratigraficheskoye polozheniye, sistematicheskii sostav, stlas rastenii]*. Magadan.

SHCZEPETOV, S.V. 1995. *Nonmarine Cretaceous Stratigraphy of North-eastern Russia [Korrelyatsiya nemorskogo mela Severo-Vostoka Rossii]*. Severo-Vostochnyi kompleksnyi nauchno-issledovatel'skiy institut Sibirskogo otdeleniya Akademii nauk, Magadan, Magadan.

SHCZEPETOV, S.V., & GOLOVNEVA, L.B. 2014. The Late Cretaceous Zarya flora of the Northern Okhotsk region and phytostratigraphy of the lower part of the Okhotsk–Chukotka volcanogenic belt section. *Stratigraphy and Geological Correlation*, **22**(4), 391–405.

SHCZEPETOV, S.V., & HERMAN, A.B. 2017. The formation conditions of the burial site of Late Cretaceous dinosaurs and plants in the Kakanaut River basin (Koryak Highlands, Northeastern Asia). *Stratigraphy and Geological Correlation*, **25**(4), 400–418.

SHCZEPETOV, S.V., HERMAN, A.B. & BELAYA, B.V. 1992. *Mid-Cretaceous flora of the right bank of the Anadyr River (stratigraphic setting, systematic composition, plant fossils atlas)*. Sev.-Vost. Kompl. Nauchn.-Issled. Inst. DVO AN SSSR, Magadan.

SMILEY, C.J. 1966. Cretaceous floras of the Kuk River area, Alaska, stratigraphic and climatic interpretations. *Geological Society of America Bulletin*, **77**, 1–14.

SMILEY, C.J. 1969a. Floral zones and correlations of Cretaceous Kukpowruk and Corwin Formations, northwestern Alaska. *American Association of Petroleum Geologists Bulletin*, **53**, 2079–2093.

Formatted: Font: Italic

Formatted: Small caps

Formatted: Small caps

Formatted: Normal

Formatted: Font: Check spelling and grammar

985 SMILEY, C.J. 1969b. Cretaceous Floras of the Chandler-Colville Region, Alaska, stratigraphy
986 and preliminary floristics. *American Association of Petroleum Geologists Bulletin*, **53**,
987 482–502.
988 SPICER, R.A. 1981. The sorting and deposition of allochthonous plant material in a modern
989 environment at Silwood Lake, Silwood Park, Berkshire. *USGS Prof. Pap.* 1143, 1–77.
990 SPICER, R.A. 1986. Comparative leaf architectural analysis of Cretaceous radiating
991 angiosperms. *In*: Spicer, R.A. & Thomas, B.A. (eds) *Systematic and Taxonomic*
992 *Approaches in Palaeobotany*. Systematics Association Special Volume, **31**, 223–233.
993 SPICER, R.A. 1987. Late Cretaceous Floras and terrestrial environment of Northern Alaska.
994 *Alaskan North Slope Geology*, **1**, 497–512.
995 SPICER, R.A. 2018. Phytopaleoaltimetry: Using Plant Fossils to Measure Past Land Surface
996 Elevation. In: Hoorn, C., Perrigo, A. & Antonelli, A. (eds) *Mountains, Climate and*
997 *Biodiversity,* (Wiley-Blackwell), 96–109.
998 SPICER, R.A., AHLBERG, A., HERMAN, A.B., KELLEY, S.P., RAIKEVICH, M.I. & REES, P.M.
999 2002. Palaeoenvironment and ecology of the middle Cretaceous Grebenka flora of
1000 northeastern Asia. *Palaeogeography Palaeoclimatology Palaeoecology*, **184**, 65–105.
1001 SPICER, R.A. & CHAPMAN, J.E. 1990. The evolution of high latitude floras, *Trends in Ecology*
1002 *and Evolution*, **5**, 279–284.
1003 SPICER, R.A. & CORFIELD, R.M. 1992. A Review of Terrestrial and Marine Climates in the
1004 Cretaceous and Implications for Modelling the Greenhouse Earth. *Geological*
1005 *Magazine*, **129**, 168–180.
1006 SPICER, R.A. & HERMAN, A.B. 2001. The Albian-Cenomanian flora of the Kukpowruk River,
1007 western North Slope, Alaska: stratigraphy and plant communities. *Cretaceous*
1008 *Research*, **22**, 1–40.

Deleted: -

Deleted: -

SPICER, R.A. & HERMAN, A.B. 2010. The Late Cretaceous Environment of the Arctic: A quantitative reassessment using plant fossils. *Palaeogeography, Palaeoclimatology, Palaeoecology*, **295**, 423–442.

SPICER, R.A., HERMAN, A.B. & KENNEDY, E.M. 2004. The Foliar Physiognomic Record of Climatic Conditions During Dormancy: CLAMP and the Cold Month Mean Temperature. *Journal of Geology*, **112**, 685–702.

SPICER, R.A., HERMAN, A.B., YANG, J. & SPICER, T.E.V. 2014. Why Future Climate Change is likely to be Underestimated: evidence from Palaeobotany. *Journal of the Botanical Society of Bengal*, **67**, 75–88.

SPICER, R.A. & PARRISH, J.T. 1986. Paleobotanical evidence for cool North Polar climates in middle Cretaceous (Albian-Cenomanian) time. *Geology*, **14**, 703–706.

SPICER, R.A. & PARRISH, J.T. 1990a. Late Cretaceous-early Tertiary palaeoclimates of northern high latitudes: a quantitative view. *Journal of Geological Society, Lond.*, **147**, 329–341.

SPICER, R.A. & PARRISH, J.T. 1990b. Latest Cretaceous woods of the central North Slope, Alaska. *Palaeontology*, **33**, 225-242.

SPICER, R.A., REES, P.M. & CHAPMAN, J.E. 1993. Cretaceous phytogeography and climate signals. In: Allen J.R.L., Hoskins, B.J., Sellwood, B.W., Spicer, R.A., Valdes, P.J. (eds), *Palaeoclimates and Their Modelling*. Royal Society/Chapman and Hall. 69–78.

SPICER, R.A., PARRISH, J.T. & GRANT, P.R. 1992. Evolution of vegetation and coal-forming environments in the Late Cretaceous of the North Slope of Alaska. In: McCabe P.J., Parrish J.T. (eds), Controls on the Distribution and Quality of Cretaceous Coals. *Geol. Soc. Amer. Spec. Pap.*, No **267**, 177–192.

SPICER, R.A. & WOLFE, J.A. 1987. Plant taphonomy of late Holocene deposits in Trinity (Clair Engle) Lake, northern California. *Paleobiology*, **13**, 227–245.

Deleted: -

Deleted: -

Deleted: -

Deleted: Tertairy

Deleted: qunatitative

SPICER, R.A., WOLFE, J.A. & NICHOLS, D. J. 1987. Alaskan Cretaceous-Tertiary floras and Arctic origins. *Paleoebiology*, **13**, 73–83.

TOMSICH, C.S., MCCARTHY, P.J., FOWELL, S.J. & SUNDERLIN, D. 2010. Paleofloristic and Paeoenevironmental information from a Late Cretaceous (Maastrichtian) flora of the lower Cantwell Formation near Sable Mountain, Denali National park, Alaska. *Palaeogeography, Palaeoclimatology, Palaeoecology*, **295**, 389–408.

UFNAR, D.F., LUDVIGSON, G.A., GONZÁLEZ, L.A., BRENNER, R.L. & WITZKE, B.J. 2004. High latitude meteoric ∂18O compositions: Paleosol siderite in the Middle Cretaceous Nanushuk Formation, North Slope, Alaska. *Geological Society of America Bulletin*, **116**, 463–473.

VASILENKO, D.V., MASLOVA, N.P. & HERMAN, A.B. 2016. Galls on the *Compositiphyllum retinerve* (Herman) Herman et Kvaček (Angiosperms) from the Turonian of the Northwestern Kamchatka Peninsula, Russia. *Paleontological Journal*, **50**(6), 653–657.

WEST, C.K., GREENWOOD, D.R. & BASINGER, J.F. 2015. Was the Arctic Eocene 'rainforest' monsoonal? Estimates of seasonal precipitation from early Eocene megafloras from Ellesmere Island, Nunavut. *Earth and Planetary Science Letters*, **427**, 18–30.

WOLFE, J.A. 1993. A method of obtaining climatic parameters from leaf assemblages: United States Geological Survey Bulletin. *United States Geological Survey Bulletin*, **2040**, 1–73.

WOLFE, J.A. & SPICER, R.A. 1999. *Fossil Leaf Character States: Multivariate Analysis*. Geological Society, London, 233–239.

YANG, J., SPICER, R.A., SPICER, T.E.V., ARENS, N.C., JACQUES, F.M.B., SU, T., KENNEDY, E.M., HERMAN, A.B., *et al.* 2015. Leaf form–climate relationships on the global stage: an ensemble of characters. *Global Ecology and Biogeography*, **24**, 1113–1125.

Formatted: Small caps

Formatted: Font: Italic

Deleted: ¶

Formatted: Font: Bold

Deleted: -

Formatted: Small caps

Formatted: Normal

Deleted: -

Deleted: -

YANG, J., SPICER, R.A., SPICER, T.E.V. & LI, C.-S. 2011. 'CLAMP Online': a new web-based palaeoclimate tool and its application to the terrestrial Paleogene and Neogene of North America. *Palaeobiodiversity and Palaeoenvironments*, **91**, 163–183.

YOUTCHEFF, J.S.J., RAO, P.D. & SMITH, J.E. 1987. Variability in two northwest Alaska coal deposits. *In*: Taileur, I. & Weimer, P. (eds) *Alaskan North Slope Geology*. Society of Economic Paleontologists and Mineralogists, Pacific Section, Bakersfield, California, **1**, 225–232.

ZAKHAROV, Y.D., BORISKINA, N.G., IGNATYEV, A.V., TANABE, K., SHIGETA, Y., POPOV, A.M., AFANANSYEVA, T.B. & MAEDA, H. 1999. Palaeotemperature curve for the Late Cretaceous of the northwestern circum-Pacific. *Cretaceous Research*, **20**, 685–697.

ZAKHAROV, Y.D., SHIGETA, Y., POPOV, A.M., VELIVETSKAYA, T.A. & AFANANSYEVA, T.B. 2011. Cretaceous climatic oscillations in the Bering area (Alaska and Koryak Upland): isotopic and palaeontological evidence. *Sedimentary Geology*, **235**, 122–131.

Deleted: -

Deleted: -

Figure Legends

Figure 1. Map of the modern North Pacific Region (NPR) showing the locations of the fossil assemblages investigated here. Vilui – Cenomanian, Arman River- Coniacian, Novaya Sibir – Turonian, Kaivayam - Coniacian, Penzhina - Turonian, Grebenka – Cenomanian, Tylpergyrgynai - Coniacian, North Slope – Coniacian. Details of the stratigraphy and sedimentary successions at each site are given in http://arcticfossils.nssi.org.cn.

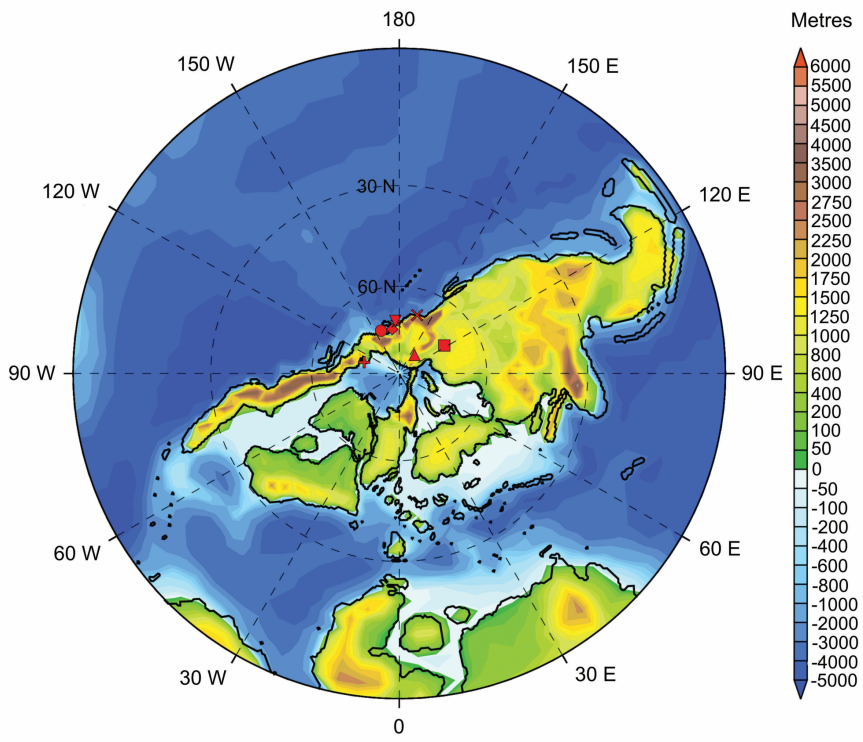

Figure 2. North polar projection of Turonian palaeogeography based on Getech Plc. reconstructions. Positions of fossil localities indicated by the following symbols: Square - Vilui River; Diagonal cross - Arman River; Triangle - Novaya Sibir (New Siberia Island); Inverted triangle - Grebenka River; Diamond - Penzhina; Star (partly hidden by the diamond)- Kaivayam; Circle - Tylpergyrgynai; Horizontal cross - North Slope.

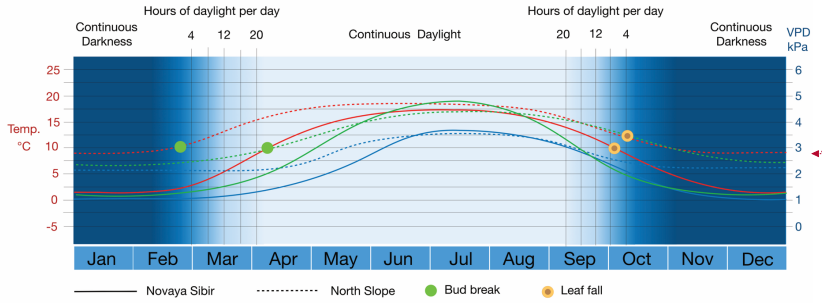

Figure 3. Light, thermal and humidity regime for fossil assemblages at palaeolatitude ~80 °N.

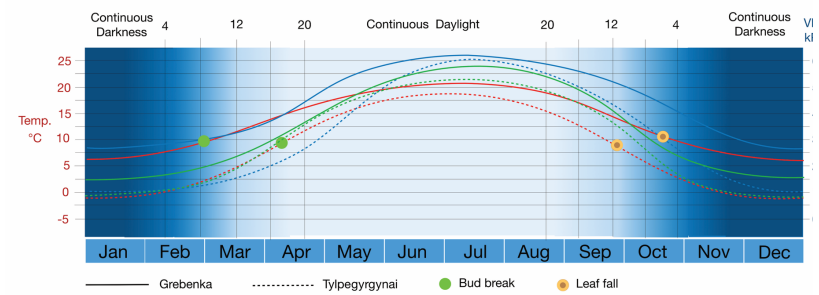

Figure 4. Light, thermal and humidity regime for fossil assemblages at palaeolatitude ~75 °N.

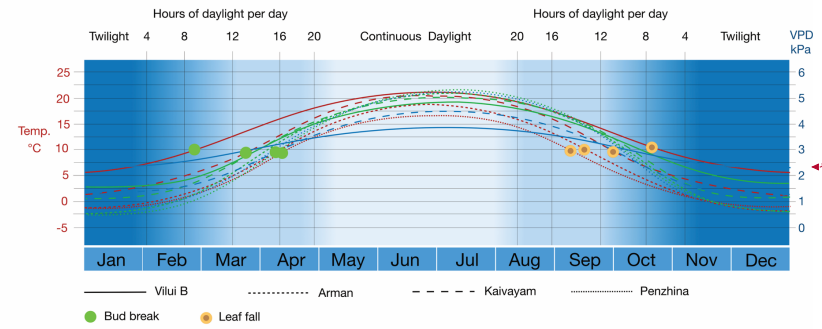

Figure 5. Light, thermal and humidity regime for fossil assemblages at palaeolatitude ~70 °N.

Formatted: Indent: Left: 1 cm

Deleted: 2

Deleted: 3

Formatted: Indent: First line: 0 cm

Deleted: 4

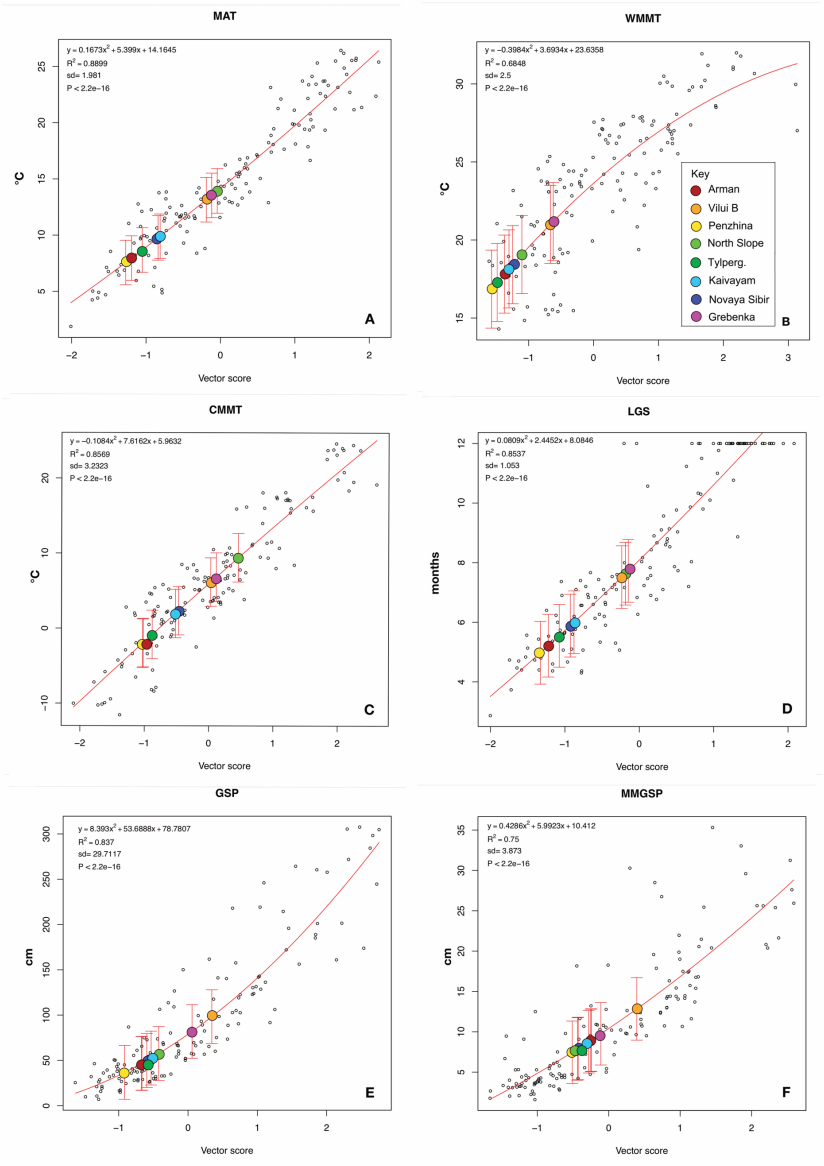

Figure 6. CLAMP regression models for the WorldClim2_3brc modern vegetation calibration sites (open black circles) and predicted climate variables for eight early Late Cretaceous

Deleted: 5

Deleted: a

Deleted: Worldclim2

fossil sites (coloured circles as in the Key shown in Fig. 5a B). Bars indicate ±1 sd. MAT - mean annual temperature, WMMT – warm month mean temperature, CMMT- cold month mean temperature, LGS – length of the growing season (temp. >10 °C), GSP – growing season precipitation, MMGSP – mean monthly growing season precipitation.

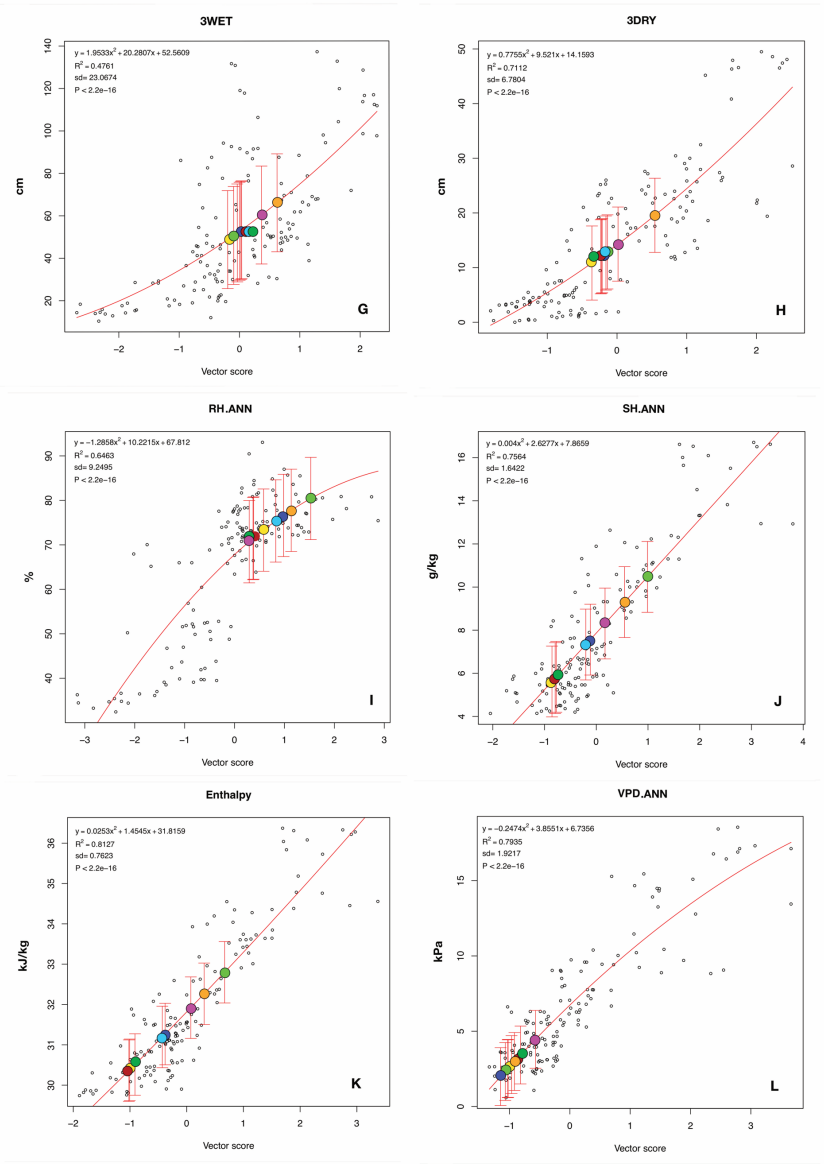

Figure 7. CLAMP regression models for the WorldClim2 3brc modern vegetation calibration sites (open black circles) and predicted climate variables for eight early Late Cretaceous

Deleted: 5b

Deleted: Worldclim2

fossil sites (coloured circles as in the Key shown in Fig. 5a B). 3WET -precipitation in the three consecutive wettest months, 3DRY - precipitation in the three consecutive driest months, RH.ANN – mean annual relative humidity, SH.ANN – mean annual specific humidity, ENTH – mean annual moist enthalpy, VPD.ANN – mean annual vapour pressure deficit.

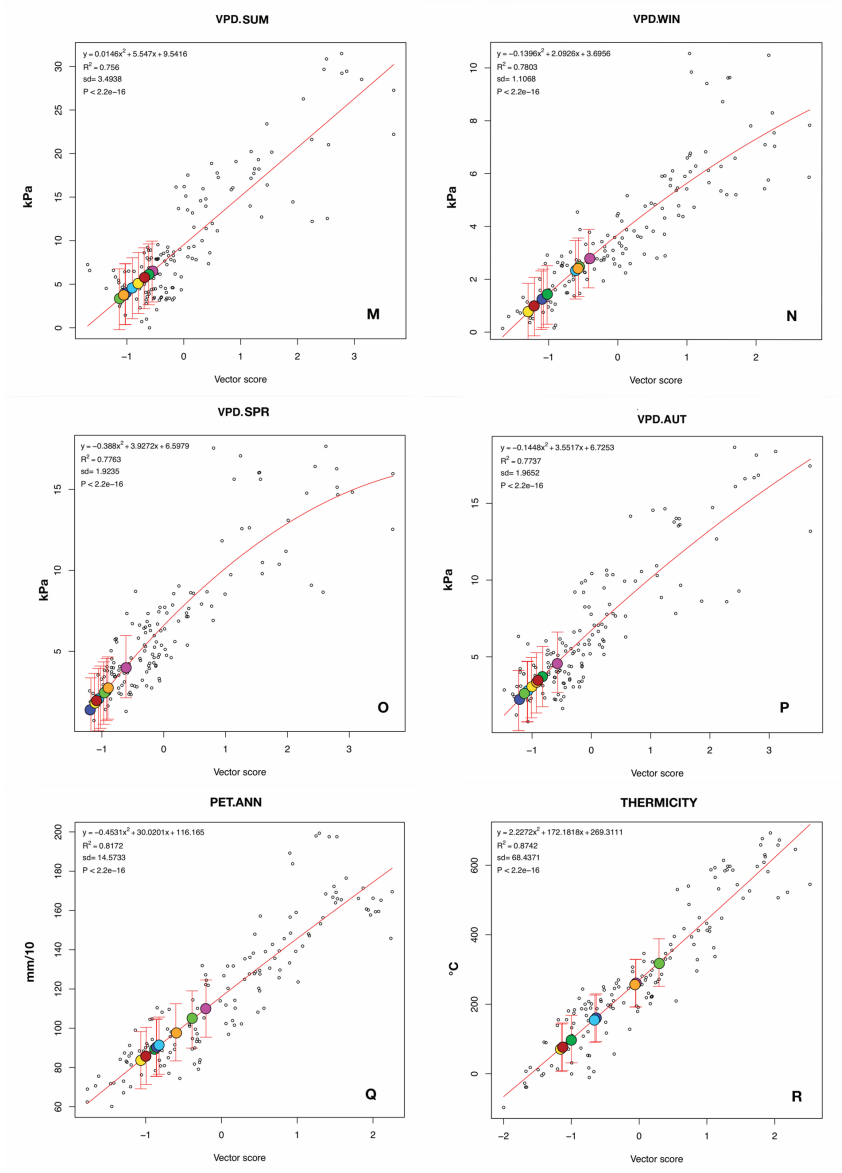

Figure 8. CLAMP regression models for the WorldClim2_3brc modern vegetation calibration sites (open black circles) and predicted climate variables for eight early Late Cretaceous

Deleted: 5c

Deleted: Worldclim2

1136 fossil sites (coloured circles as in the Key shown in Fig. 5a B). VPD.SUM - mean summer
1137 vapour pressure deficit, VPD.WIN - mean winter vapour pressure deficit, VPD.SPR - mean
1138 spring vapour pressure deficit, VPD.AUT – mean autumn vapour pressure deficit.

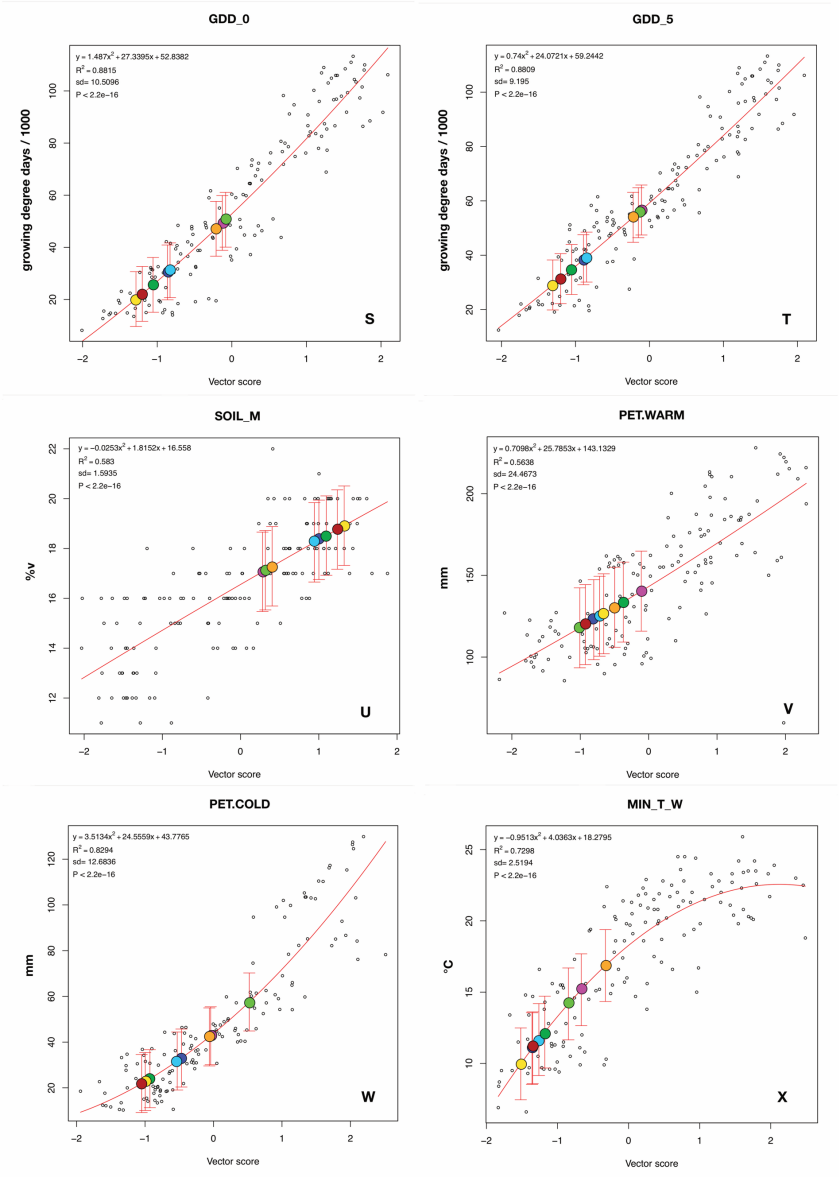

Figure 9. CLAMP regression models for the WorldClim2_3brc modern vegetation calibration sites (open black circles) and predicted climate variables for eight early Late Cretaceous

Deleted: 5d

Deleted: Worldclim2

fossil sites (coloured circles as in the Key shown in Fig. 5a B). GDD_0 - growing degree days when temperatures are above freezing, GDD_5 - growing degree days when temperatures are above +5°C, SOIL_M - derived soil moisture capacity, PET.WARM - potential evapotranspiration during the warmest month, PET.COLD - potential evapotranspiration during the coldest month, MIN_T_W - minimum temperature of the warmest month.

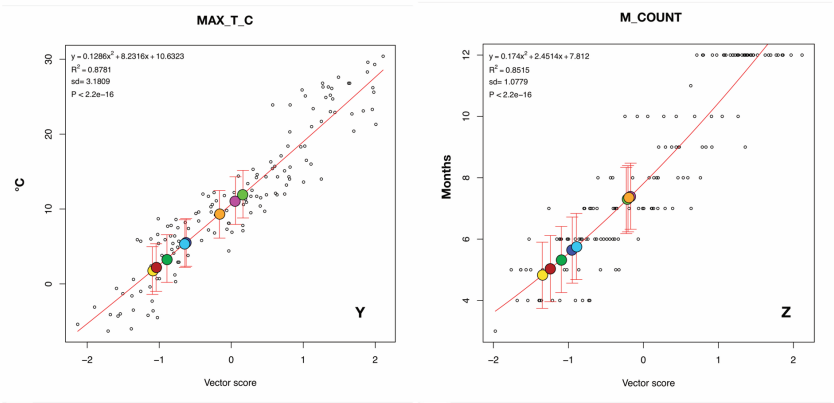

Figure 10. CLAMP regression models for the WorldClim2_3brc modern vegetation calibration sites (open black circles) and predicted climate variables for eight early Late Cretaceous fossil sites (coloured circles as in the Key shown in Fig. 5a B). MAX_T_C - maximum temperature during the coldest month, M_COUNT - number of months where the temperature is above +10°C.

Deleted: 5e

Deleted: Worldclim2

Table legends

Table 1. Summary of CLAMP environmental variables, their acronyms, descriptions and units, derived from WorldClim2 gridded data at ~ 1 km spatial resolution.

Table 2. Summary of temperature-related CLAMP-derived metrics for early Late Cretaceous plant assemblages from the North Pacific Region. Values obtained by a CLAMP calibration based on WorldClim2_3br and GRIDMet_3br (in parentheses) gridded climate data. MAT - mean annual temperature, WMMT - warm month mean temperature, CMMT 0- cold month mean temperature, MIN_T_W - minimum temperature of the warmest month, MAX_T_C - maximum temperature of the coldest month, THERM. - compensated thermicity index: sum of mean annual temp., min. temp. of coldest month, max. temp. of the coldest month, x 10, with compensations for better comparability across the globe, GDD_0 - sum of mean monthly temperature for months with mean temperature greater than 0°C multiplied by number of days, GDD_5 - sum of mean monthly temperature for months with mean temperature greater than 5 °C multiplied by number of days, LGS - length of the growing season when mean temperatures are above 10 °C, M_COUNT - count of the number of months with mean temp greater than 10 °C.

Table 3. Summary of precipitation, soil moisture and moist enthalpy CLAMP-derived metrics for early Late Cretaceous plant assemblages from the North Pacific Region. Values obtained by a CLAMP calibration based on WorldClim2 and, in parentheses, GRIDMet_3br gridded climate data. GSP – precipitation during the growing season, MMGSP – mean monthly precipitation during the growing season, 3WET – precipitation during the three consecutive wettest months, 3DRY – precipitation during the three consecutive driest months, SOIL_M -

Deleted: ¶

Formatted: Indent: Left: 0.25 cm, First line: 0 cm

Deleted: ¶

Deleted: 1

Deleted: 2

Derived available soil water capacity (volumetric fraction) predicted using the global compilation of soil ground observations (ftp://ftp.soilgrids.org/data/recent/AWCh1_M_sl2_250m.tif), ENTH-annual mean moist enthalpy.

Table 4. Summary of humidity metrics, soil moisture and moist enthalpy CLAMP-derived metrics for early Late Cretaceous plant assemblages from the North Pacific Region. Values obtained by a CLAMP calibration based on WorldClim2 and GRIDMet_3br (in parentheses) gridded climate data. RH.ANNUAL - annual mean relative humidity, SH.ANNUAL - annual mean specific humidity, VPD.ANN - annual mean vapour pressure deficit, VPD.SUM - mean VPD for the summer quarter, VPD.WIN - mean VPD for the winter quarter, VPD.SPR - mean VPD for the spring quarter, VPD-AUT - mean VPD for the autumn quarter, PET.ANN - annual mean potential evapotranspiration, PET.WARM - mean potential evapotranspiration for the warmest quarter, PET.COLD - mean potential evapotranspiration for the coldest quarter.

Deleted: 3

Table 1. CLAMP Climate Variables and Descriptions

Formatted Table

Name	Acronyn	Description	Units
Mean annual temperature	MAT	Mean temperature throughout the year	°C
Warm month mean temp.	WMMT	Average temperature of the warmest month	°C
Cold month mean temp.	CMMT	Average temperature of the coldest month	°C
Length of the growing season	LGS	Number of months when temperatures are ≥ 10°C	Number
Growing season precipitation	GSP	Total precipitation during the growing season (temperature ≥ 10°C)	cm
Mean monthly growing season precipitation	MMGSP	Average precipitation per month during the growing season	cm
Precipitation during the three wettest months	3-WET	Average precipitation during the three consecutive wettest months	cm
Precipitation during the three driest months	3-DRY	Average precipitation during the three consecutive driest months	cm
Relative humidity	RH.ANN	Average annual relative humidity	%
Specific humidity	RH.ANN	Average annual specific humidity (the amount of water in a kg of dry air)	g/kg
Enthalpy	ENTH	Average annual moist enthalpy (energy per kilogram of air)	kJ/kg
Minimum temperature of the warmest month	MIN_T_W	Lowest daily temperature during the warmest month	°C
Maximum temperature of the coldest month	MAX_T_C	Warmest daily temperature during the coldest month	°C
Compensated Thermicity Index	THERM	Sum of mean annual temp., min. temp. of coldest month, max. temp. of the coldest month, x 10, with compensations for better global comparability	°C
Growing degree days 0	GDD_0	Sum of mean monthly temperature for months with mean temperature > 0°C multiplied by the number of days this occurs	Number
Growing degree days 5	GDD_5	Sum of mean monthly temperature for months with mean temperature > 5°C multiplied by number of days this occurs	Number
Month count	M_COUNT	Count of the number of months when the temperature > 10°C	Number
Soil Moisture	SOIL_M	Derived available soil water capacity (volumetric fraction) at 7 standard depths predicted using the global compilation of soil ground observations.	%v
Mean annual vapour pressure deficit	VPD. ANN	Average annual vapour pressure deficit	hPa
Mean summer vapour pressure deficit	VPD.SUM	Average vapour pressure deficit during the three summer months	hPa
Mean winter vapour pressure deficit	VPD.WIN	Average vapour pressure deficit during the three winter months	hPa
Mean spring vapour pressure deficit	VPD.SPR	Average vapour pressure deficit during the three spring months	hPa
Mean autumn vapour pressure deficit	VPD.AUT	Average vapour pressure deficit during the three autumn months	hPa
Potential evapotranspiration (PET)	PET.ANN	The ability of the atmosphere to remove water through evapo-transpiration, given unlimited water supply, averaged over the year	mm/month
Mean PET of the warmest month	PET.WARM	PET averaged over the warmest month	mm/month
Mean PET of the coldest month	PET.COLD	PET averaged over the coldest month	mm/month

Table 2. Temperature-Related Metrics

LOCALITY	AGE	MAT (°C)	WMMT (°C)	CMMT (°C)	MIN_T_W (°C)	MAX_T_C (°C)	THERM. (°C)	GDD_0	GDD_5	LGS (months)	M_COUNT (months)
Vilui "B"	Cenomanian	13.1 (12.8)	21 (21)	6.2 (5.3)	16.9	9.3	260	47124	53955	7.5 (7.4)	7.3
Grebenka	Cenomanian	13.5 (12.9)	21.2 (20.8)	6.8 (5.9)	15.2	11.1	261	49372	56645	7.7 (7.4)	7.4
Tylpergyrg.	Coniacian	8.7 (8.4)	18.4 (18.8)	-0.8 (-1.6)	11.7	3.4	100	25612	34745	5.5 (5.4)	5.3
Novaya Sibir	Turonian	9.8 (9.2)	17.3 (17)	2.4 (1.1)	11.0	5.5	161	30389	38347	5.9 (5.8)	5.6
North Slope	Coniacian	13.9 (13.3)	19.1 (19.1)	9.4 (7.9)	14.2	12.0	320	50590	55643	7.6 (7.6)	7.3
Arman	Cenomanian	8.0 (8.2)	17.8 (18.7)	-1.9 (-2)	11.1	2.2	78	22150	31392	5.2 (5.3)	5.0
Kaivayam	Coniacian	9.9 (9.6)	18.1 (18.3)	1.9 (1.1)	12.2	5.4	158	31201	39311	6.0 (6.0)	5.8
Penzhina	Turonian	7.6 (7.7)	16.9 (17.7)	-2 (-2.4)	10.0	1.8	75	20161	29057	5.0 (4.9)	4.8
Standard Deviation		2.0 (1.1)	2.5 (1.4)	3.2 (1.9)	2.5	3.2	68	10510	9195	1.1 (0.7)	1.1

Table 3. Precipitation, Soil Moisture and Enthalpy Metrics

LOCALITY	AGE	GSP (cm)	MMGSP (cm)	3WET (cm)	3DRY (cm)	SOIL_M (%V)	ENTH (kJ/kg)
Vilui "B"	Cenomanian	98 (105)	13 (13.5)	66 (62)	20 (21)	17.3	323 (324)
Grebenka	Cenomanian	82 (82)	10 (9)	60 (58)	14 (15)	17.1	319 (317)
Tylpergyrg.	Coniacian	50 (48)	9 (9)	53 (49)	12 (13)	18.5	305 (303)
Novaya Sibir	Turonian	47 (54)	8 (8.2)	52 (50)	12 (15)	18.4	313 (310)
North Slope	Coniacian	58 (79)	7 (9)	51 (53)	13 (13)	17.1	328 (326)
Arman	Cenomanian	47 (48)	9 (9)	53 (48)	12 (14)	18.8	303 (304)
Kaivayam	Coniacian	53 (60)	9 (9)	53 (52)	13 (15)	18.2	312 (310)
Penzhina	Turonian	37 (38)	8 (8)	49 (47)	11 (14)	18.9	304 (304)
Standard Deviation		30 (30)	4 (3)	23 (14)	7 (3)	1.6	8 (5)

Table 4. Humidity Metrics

LOCALITY	AGE	RH.ANNUAL (%)	SH.ANNUAL (g/kg)	VPD.ANN (kPa)	VPD.SUM (kPa)	VPD.WIN (kPa)	VPD.SPR (kPa)	VPD. AUT (kPa)	PET.ANN (mm)/10	PET.WARM (mm)	PET.COLD (mm)
Vilui "B"	Cenomanian	78 (80)	9.3 (9.6)	2.8	3.8	2.4	2.7	3.0	97.9	119.9	42.3
Grebenka	Cenomanian	71 (73)	8.3 (8)	4.5	6.5	2.8	4.1	4.7	110.0	140.3	42.8
Tylpergyrg.	Coniacian	71 (71)	5.8 (5.3)	3.4	6.1	1.3	2.6	3.7	90.1	133.7	24.0
Novaya Sibir	Turonian	77 (77)	7.6 (7)	2.0	3.9	1.2	1.4	2.1	90.0	122.9	33.0
North Slope	Coniacian	80 (80)	10.5 (10.1)	2.3	3.3	2.5	2.4	2.2	104.4	117.9	57.6
Arman	Cenomanian	72 (74)	5.6 (5.8)	3.0	5.7	1.0	2.2	3.3	85.9	130.5	21.9
Kaivayam	Coniacian	75 (76)	7.3 (7)	2.5	4.5	1.4	2.0	2.7	91.1	125.0	31.7
Penzhina	Turonian	73 (75)	5.8 (5.8)	2.5	5.1	0.7	1.7	2.7	83.7	126.5	22.8
Standard Deviation		9 (5)	1.6 (1)	1.9	3.5	1.1	1.9	2.0	14.6	24.5	12.7

Deleted: 1
Formatted Table
Deleted: 2
Formatted Table
Deleted: 3
Formatted Table